Summer 7-15-2017

CHARACTERIZATION OF METHODS FOR SURFACE CHARGE REMOVAL FOR THE REDUCTION OF ELECTROSTATIC DISCHARGE EVENTS

Khandakar Nusrat Islam
University of New Mexico

Khandakar Nusrat Islam
Candidate

Electrical and Computer Engineering
Department

This thesis is approved, and it is acceptable in quality and form for publication:

Approved by the Thesis Committee:

Dr. Mark Gilmore, Chairperson

Dr. Edl Schamiloglu

Francis J. Martinez

_____

_____

_____

_____

_____

_____

CHARACTERIZATION OF METHODS FOR SURFACE CHARGE REMOVAL
FOR THE REDUCTION OF ELECTROSTATIC DISCHARGE EVENTS

by

KHANDAKAR NUSRAT ISLAM

B.S. IN ELECTRICAL AND ELECTRONIC ENGINEERING
EASTERN UNIVERSITY DHAKA, BANGLADESH
2011

THESIS

Submitted in Partial Fulfillment of the
Requirements for the Degree of

Master of Science
In
Electrical Engineering

The University of New Mexico
Albuquerque, New Mexico

July 2017

Dedication

To my dad, who I lost when I was only 15, and to my mom – they are my strength and always encourage me to believe in myself.

me to the world of research and always encouraged me to be excellent in my endeavors. He was of great assistance in helping me begin my journey of higher study in the US.

This thesis would not have been possible without the help, support and patience of my lab mates Karin Fulford, Ralph Kelly, Scott Betts, and other lab members. It would have been a lonely lab without them.

I would like to thank Kirt Alan Nakagawa, a good friend, who provided an apparatus for my thesis work. He, along with former classmate and ex-business partner Chandan Qumar Hawlader, an MS student at the University of Manitoba, Canada, were always willing to help and offer suggestions, encouragement, practical and scientific advice.

I would like to thank my host family, Schea and Peter Freimanis, who treated me like family and for their love, encouragement throughout the past two years.

Last but not the least, I would like to thank my Mom, my brother and five sisters for all their love, support, and encouragement throughout the journey of my life. I would like to offer a very special thanks to my two sisters, Khandoker Nasrin Ismet Ara and Khandoker Nilufa Jahan, who taught me Math, Science and English until I entered college. Without their guidance and inspiration, I would not be where I am today.

CHARACTERIZATION OF METHODS FOR SURFACE CHARGE REMOVAL

FOR THE REDUCTION OF ELECTROSTATIC DISCHARGE EVENTS

By

Khandakar Nusrat Islam

B.Sc., in Electrical and Electronic Engineering, Eastern University, 2011

M.S., in Electrical Engineering, University of New Mexico, 2017

Abstract

Electrostatic discharge (ESD) from charged dielectric materials used in explosive environments presents a significant hazard. In order to investigate dielectric surface charging and methods of removing this charge in a controlled manner, a test stand has been built to study the behavior of several common dielectric materials used in such environments. A corona discharge source of the type used in electrostatic printing technology has been employed at normal laboratory temperatures and at low and high relative humidity in a controlled manner.

Dielectrics tested included black/semi-black/yellow Kapton, Lexan, Delrin, and red Adiprene with surface potentials (V_{diel}) ranging from -1 kV to -15 kV. Uniform charging and discharging of individual dielectric samples of varying thickness have been characterized by spatial scans of the surface potential at relatively low voltages. At higher charging voltages, the surface potential is found to decay or increase with time in complex ways, showing a dependence on the magnitude of the surface potential V_{diel}, as well as two characteristic time constants, t_d (τ_1, τ_2) in some cases. The initial discharge of

V_d (t_d) is rapid, while the subsequent discharge of surface potential is found to be much slower. The decay time constant(s) is(are) found to be a nonlinear function of the surface voltage, V_{diel}. A conductive brush and a static dissipative brush grounded on the metal plate is found the most effective method to remove the majority (typically 80-90%) of the surface charge, Q_s. Additionally, it was found that localized discharging results in a constant electric field gradient, ∇E on the dielectric samples in 2D. A limited number of experiments have been conducted if there is any correlation between the tendency of a dielectric to charge more and the surface resistivity of the dielectric material. Experimental results from surface resistivity and chargeability on all tested dielectric at -10 kV show that the semi black/yellow Kapton charges even more than that materials have low resistivity than Lexan/Delrin. Even after 10 mins, yellow Kapton still retain a significant amount of charge than Delrin. An investigation on yellow Kapton with 0.127 mm thickness also shows that the higher relative humidity affects the surface resistivity significantly.

TABLE OF CONTENTS

LIST OF FIGURES

LIST OF TABLES

CHAPTER 1: INTRODUCTION

1.1 Background of the study

Electrostatic discharge (ESD) is now a major concern in modern electronics. It is not surprising that the first electrostatic experiment was recorded by Thales (640 - 546 B.C), a Greek philosopher from Miletus [1]. Since then electrostatic discharge (ESD) is now a widespread issue in many industries (i.e. explosives, printing, textiles, painting, petrochemical, pharmaceutical, agriculture, plastics, etc.). Thousands of companies and many national laboratories and other research institutions pay attention to static control today. Despite a great effort over last few decades, electrostatic discharge still affects packaging, manufacturing, handling, product quality, profitability and so on. The cost of damaged devices can be from only a few cents for a simple device to thousands of dollars for complex integrated circuit [2]. This thesis is primarily addressing the interruption effects of electrostatic discharge (ESD) to explosive materials handling.

ESD is defined as "the transfer of electrostatic charge between bodies at different electrostatic potentials caused by direct contact or induced by an electrostatic field" [3]. It may stop the normal operation of a device or can cause equipment malfunction or failure. Perhaps the human body is the most common ESD source, but other sources (i.e. humidity, room temperature, personnel clothing/shoes) also generate ESD [4]. Certain types of materials (e.g. dielectric-metal, metal-metal or dielectric-dielectric) can also cause ESD when they come into contact and separate, which can result in triboelectric charging. Thus, static electricity (or an imbalance of electrical charges) is often created that leads to an ESD event. The amount of charge generated by triboelectric charging is

affected by many factors including contact area, speed of separation, relative humidity, chemistry of the materials, and surface work function [5]. Typical cases of triboelectric charge generation and the resulting voltage levels are shown in Table 1.

Table 1: Examples of triboelectric charge generation – typical voltage levels [6].

Means of Generation	10 - 25% RH	65 - 90% RH
Walking Across Carpet	35,000V	1,500V
Walking Across Vinyl Tile	12,000V	250V
Worker at a Bench	6,000V	100V
Poly Bag Picked up from Bench	20,000V	1,200V
Chair with Urethane Foam	18,000V	1,500V

These triboelectric charging materials, lumped together, are known as a triboelectric series. This series defines materials related with positive or negative charges. Positive charges stored mainly on human skin or animal fur, for example, while negative charges are more common to synthetic materials (i.e. Styrofoam or plastics) [7]. The amount of electrostatic charge on any item can accumulate based on its capacity to store a charge. A typical triboelectric series is shown in Table 2. This table is used only as a general guide because there are many variables involved that cannot be controlled well enough to ensure repeatability [8].

Electrostatic discharge occurs in many ways and often creates a spark. One of the most common ESD events is human contact with sensitive devices and ESD voltage levels can exceed 4 kV [9]. Many of examples can be seen over last few decades. Many national

laboratories and some companies have been working on

Table 2: Typical triboelectric series [10]**.**

Positively $^+$ charged materials
Rabbit fur Glass Mica Human Hair Nylon Wool Fur Lead Silk Aluminum
Negatively $^+$ charged materials
Paper Cotton Steel Wood Amber Sealing Wax Nickel, copper Brass, silver Gold, platinum Sulfur Acetate rayon Polyester Celluloid Silicon Teflon

controlling ESD in explosive environments. An ESD in an explosive environment may result in fire or explosion, causing considerable physical damage, human injury, or loss of life [11]. Some of these environments often use dielectric materials for packaging, assembling, and, handling of explosive materials. For example, a number of groups at Los Alamos National Laboratory (LANL) have been working on characterization of dielectric materials in order to eliminate ESD. This thesis refers to the LANL project with the goal of characterizing dielectric materials.

3

A dielectric material (dielectric for short) is an electrical insulator where the constituent atom or molecules can be polarized by the presence of an electric field and having an electrostatic field within them under the state of polarization [12]. Unlike conductor materials, insulators have extremely high resistance (e.g. $> 10^{11}$ ohms). Thus, charges remain on the surface of the dielectric unless it is grounded or contacts another material, including another dielectric, so that the charges can bleed off. In addition, a sudden static charge on the materials may also give rise to an unwanted mechanical force which can initiate an explosion [13]. Some specific dielectric materials or plastic sheets may become a source of ESD as a consequence of the explosive initiator.

There remains a question of how to avoid ESD in packaging and handling dielectric materials in an explosive environment. Earth grounding or the use of conductive footwear may not be helpful in avoiding ESD hazards while workers handle and assemble explosive materials. Some other safety issues also related to detonator handling, assembly, and disassembly, as well as transportation and maintenance, should be considered since these risks include high explosive violent reactions (HEVR) and nuclear detonations [14].

This project was supported by Los Alamos National Laboratory (LANL) towards the goals of characterizing the surface charge of common dielectrics, and to design a method/tool to remove the static charge from the surface of these materials. This thesis reports the findings of a study of surface charge generation on several dielectric materials and efforts to develop a method for surface charge removal for the reduction of the ESD events. Broadening the scope of application outside of the LANL explosive center,

beneficial uses could be found in other applications (e.g. in the photocopying industry or Xerography, Van de Graff generators, static dischargers, electrostatic precipitators, paint sprayers, sandpaper and grit cloth manufacture, separation of mineral ores, electrostatic atomization, etc.).

1.2 Prior work and problem statement

There is now ample research on surface charge characterization of dielectric or polymer sheet conducted by many laboratories (e.g. LANL [15], NASA [16]) and other researchers D. K. Davies 1969 [17], Pierre Jay' Dccines 1970 [18], EA Baum, T J Lewis and R Toomer 1977 [19], A.R Blythe and G.E Carr 1981 [20], Tetsuji Oda and Yuko Ito 1990 [21], Jose A. Giacometti and Osvaldo N. Oliveira Jr. 1992 [22], Norbert Gibson 1997 [23]. However, little or no research appears to have been reported for surface charge removal methods that avoid ESD events.

Tetsuji Oda and Yuko Ito studied ESD phenomena on charged thin polymer films (i.e. FEP or PTFE Teflon) at surface potentials from 1 to 5 kV in both polarities [21]. In this study, dielectric film was charged by a corona or some other similar methods to produce a uniformly charged surface. A 5mm diameter based grounded sphere electrode approached the charged surface until the surface discharge occurred. The results of this experiment reported one-dimensional potential profiles after the discharge and the charge transfer from the charged surface to the ground sphere electrode. The grounded sphere electrode approached the surface and stopped after the discharge without contacting the dielectric film. For a better understanding of the ESD phenomenon, the authors measured the electrostatic discharge current waveform by using a voltage divider and a discharge gap distance.

Francis J. Martinez of LANL conducted three triboelectric charge transfer experiments – triboelectric charging, drill experiment, and, aggressive charging - to generate electrostatic charge and an associated electric field on different materials. The materials included aluminum, Red HE Adiprene^{TM}, Black HE Adiprene^{TM}, Gray HE PVC, Lexan, and, Teflon – all used within the DOE Weapons Complex. A Simco FMX-003 electric field meter was used to measure the electric field of each tested material. The first experiment was triboelectric charging where a piece of aluminum was wrapped with fabric (used as the charge transfer tool) and it had a string attached to it. The end of this string was connected to a spool (cylindrical device). This device was attached to a variable speed controlled drill to drag the charging tool in a linear manner across the material surface. This experiment generated lower electric field < 2.5 kV/in. The second experiment for generating electric field, was the "Drill experiment", where the charging tool was dragged with a higher velocity and a higher electric field < 4.5 kV/in was generated. The third experiment was "Aggressive charging" to observe any relationship between the surface resistivity and triboelectric effect. A foam block was wrapped with the charging fabric material and it was manually rubbed aggressively against the tested material back and forth (for 5 seconds with a subjectively uniform force). This experiment generated a large electric field < 14 kV/in. The final experiment used three brushes to remove the charge from the surface. However, from the above experiments, it was shown that there was no direct correlation between the magnitude of the change of the electric field and the order of the magnitude of the surface resistivity of the material under test. Lexan showed some significant triboelectric effects at three experiments and an ungrounded brush removed surface charge between 5% and 40%, but the grounded

brush removed almost 90% surface charge. This conclusion leads to this thesis work. Thus, we focused on better charging method in order to improve surface charge uniformity, as well as some other new materials for understanding their properties, have also been explored.

1.3 Objectives of the study

- Explore dielectric materials.

- Develop an improved understanding of dielectric charging and discharging in explosive environments.

- Find a method to eliminate electrostatic discharge (ESD) due to charged dielectrics in such environments.

- Develop an ESD-free method for discharging dielectric materials.

- Explore new materials to find a correlation between the tendency of a dielectric to charge and its surface resistivity. (Martinez explored few materials).

- Characterize the relationship between the humidity levels and the tendency of a dielectric to charge.

1.4 Thesis overview

This thesis is devoted to the subject of measurement techniques applied to the electrical behavior and characterization of dielectric materials. An attempt was made to provide a complete description of each experiment and to perform measurements accurately. However, despite the complexity of the available experimental setup and associated equipment for dielectric surface charging, some degree of brevity had to be maintained.

Consequently, the more accepted test data and all practical experiments have been described in section 3. All experiments are subjected to the higher sensitivity and stability of the experimental setup and associated all equipment (i.e. power supplies, E-field meter etc.). Nevertheless, the results of the overall project work permit us to examine the dielectric surface charge phenomena in greater detail and reduce the static charge from the dielectric surface.

The contents of this thesis are divided into five chapters. The first chapter introduces the ESD concern in explosives environment. Chapter 2 treats the experimental arrangement. The associated apparatus and insulating materials are described, details of the corona charging mechanism for uniformity are given, and the brush tool experiments are given. Chapter 3 describes various test methods and procedures of the surface charge generation and measurements (i.e. uniform charging and discharging, passive discharging versus time; localized brushing, influence of surface resistivity, humidity variation). Test methods are described using various dielectric materials such as Delrin, Lexan, black/semi-black/yellow Kapton, and red Adiprene have been performed in an ambient humidity and temperature controlled environment and high voltage sources. Chapter 4 presents a brief discussion of surface charge calculations which includes capacitance and surface resistivity measurements.

Finally, chapter 5 contains overall conclusions on dielectric surface charging and effectiveness of the brush tool for surface charge removal in regards to dealing with ESD. Possible future work is outlined at the end of this chapter which propose to establish an automated system to run the corona source, the electric field meter, and a brush tool.

CHAPTER 2: EXPERIMENTAL ARRANGEMENT

2.1 Surface charge generation

Corona charging is one of the earliest methods to form an electrostatic image on a dielectric sheet, where electrons are deposited directly onto the dielectric substrate by an accelerating field [24]. In order to investigate dielectric surface charging and methods of removing the charge in detail, and in a controlled way, a test stand has been constructed using a corona charging source, as shown in Figure 1.
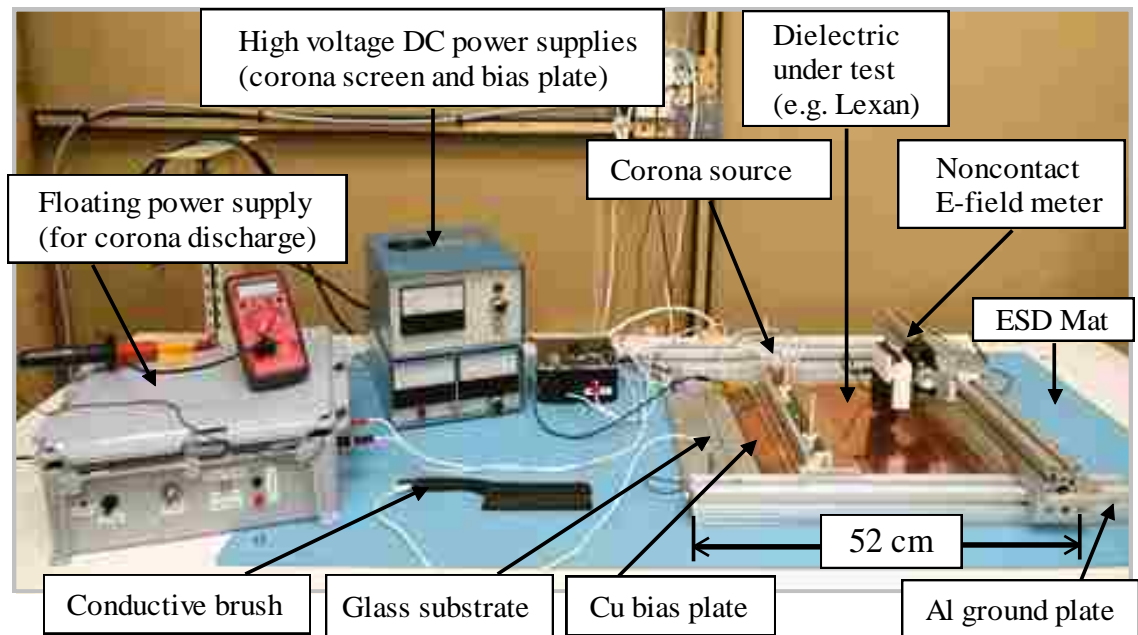
Figure 1: A test set up for surface charge measurements.

The test stand is built around a corona discharge source of the type used in photographic printing technologies. The corona charging source was taken from a Tektronix Phaser 6120 printer. A dielectric sample is placed on the Al plate and the source sits on a height-adjustable 8020 sliding rail with a spacing of (typically) 1.5 - 5 mm above the dielectric

sample (*cf*. Figure 1). A noncontact electric field (E-field) meter, model M282, manufactured by Monroe, is mounted on an aluminum sliding rail which allows motion of the detector in the x-, y-, and z-directions. The entire assembly resides on a ½ in. thick aluminum mounting plate. An earth grounded static-safe workbench with a static dissipative table mat is also used for ESD control and the Al plate is earth grounded. Relative humidity of minimum 16% and maximum 71%, and a temperature of 20°C – 24°C were maintained. Furthermore, the operator was also grounded by a wrist-strap while handling the charged dielectric materials.
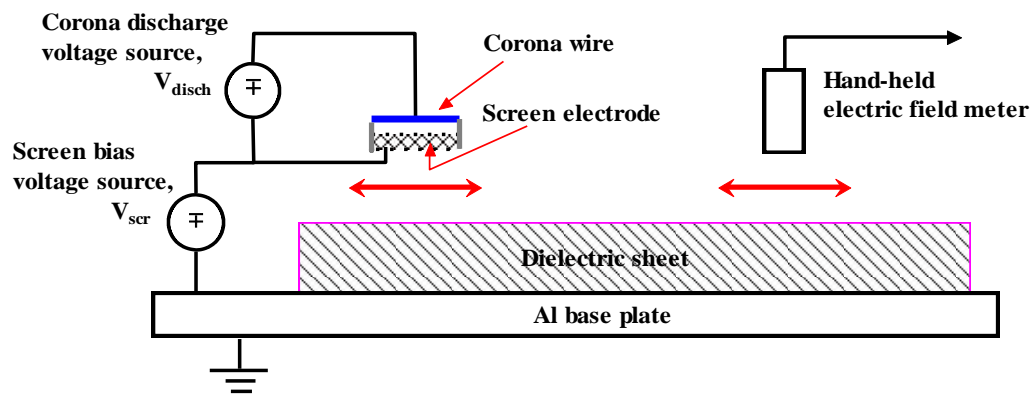
Figure 2: A schematic test stand for controlled charging and discharging of dielectric material

2.1.1. Negative charging by corona source

The corona source operated routinely and reliably to charge the tested dielectric materials negatively. As shown in   Figure 2, the corona source is placed a few mm (1.5 – 5 mm) above the sheet of dielectric which rests on the aluminum conductor plate. The corona source has a thin corona wire which is insulated by black plastic and completely separated from the corona screen electrode (*cf*. Figure 3a). This corona source operates two dc power supplies (V_{disch}, V_{scr}) as shown in   Figure 2. A floating power supply,

(typically) $V_{disch} \sim$ -1 kV to -6 kV is applied between the corona wire (corona thin wire inside the source) and corona screen grid electrode; another power supply, $V_{disch} \sim$ -600 V to -15 kV is used to bias the screen electrode with respect to the Al ground plate. Both applied voltages (V_{disch}, V_{scr}) remain constant when the corona source passes over the surface of the sample (*cf.* Figure 3b).
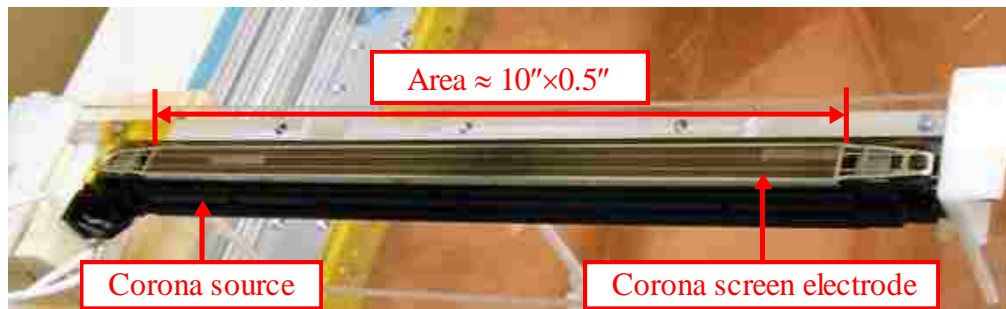
(a)
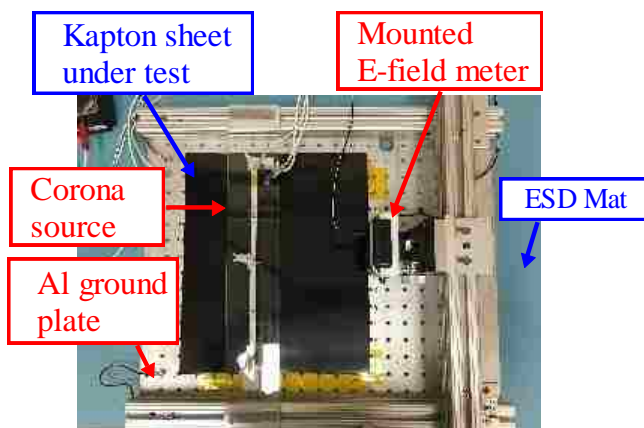
(b)

(c)

(d)

Figure 3: Upper (a): Corona source from Tektronix Phaser 6120 printer. Lower Left (b): Corona charging process on dielectric material. Lower Right (c), (d): Corona discharge plasma.

The screen voltage, V_{scr} produces an electric field between the screen electrode and the Al ground plate through the dielectric. A corona discharge plasma (*cf.* Figure 3c and Figure 3d) is created as $V_{disch} \approx$ -3 kV is applied between the corona electrode and screen grid electrode. This plasma is the source of free electrical charges which are accelerated by the electric field produced by V_{scr}. The free electrical charges drift toward the dielectric and charge the surface of the dielectric until the electric field is reduced to near zero so that no free charge can be drawn from the corona source (*cf.* Figure 4). Hence, the potential difference between the dielectric surface and the screen electrode will be zero, $V_{diel} \sim V_{scr} = 0$ or $V_{diel} \approx V_{scr}$. It is expected that the dielectric surface is charged uniformly in the area covered by the source.

Figure 4: Corona charging schematic for dielectric surface charging.

The available screen bias voltage source, V_{scr} was limited to -10 kV. Therefore, as shown in Figure 5, a second set up has been used to achieve the dielectric surface voltage, $V_{diel} >$ -10 kV. An additional positive copper bias plate backing a glass plate insulator is placed under the tested sample. The copper plate is biased to a few kV voltages, ($V_{plate} \approx$ -1 kV to above) with respect to the Al plate and thus the resulting charging bias voltage, $V_{diel} \approx$

12

$V_{scr} - V_{plate}$. For example, if screen bias voltage, V_{scr} = -10 kV and V_{plate} = +5 kV, resulting surface voltage of dielectric, $V_{diel} \approx$ -15 kV.
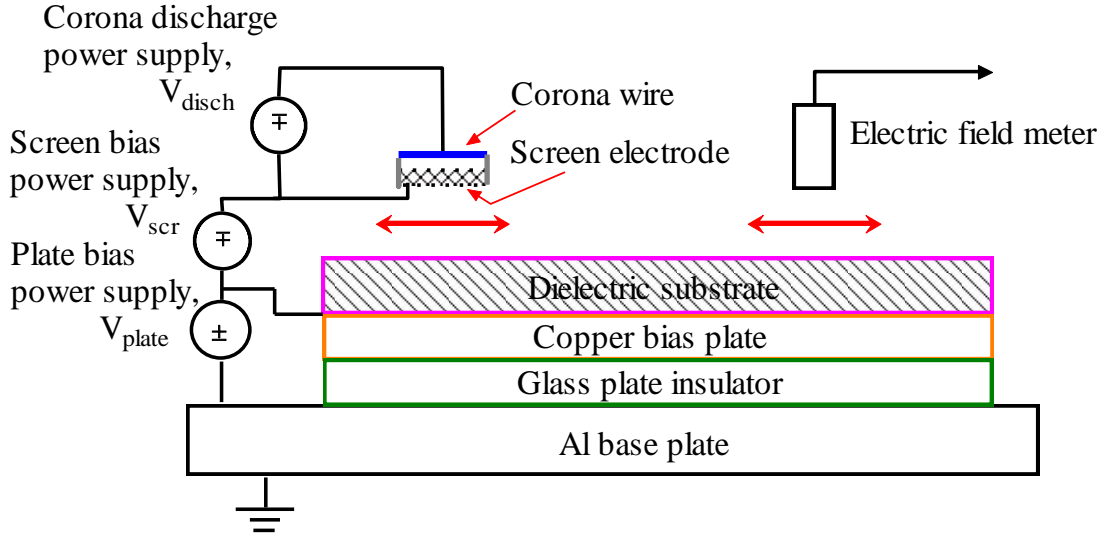
Figure 5: Corona charging test stand with additional positive copper bias plate.

2.1.2. Positive charging by corona source

Unfortunately, the tested materials were not charged effectively with positive screen biasing. Several attempts were made by biasing screen electrode with different positive high voltages ($+V_{scr}$) to charge the materials under test. An additional attempt was made to obtain surface charge with positive polarity by biasing the Al base plate (V_{plate}), more negative than the screen voltage (V_{scr}), such as $V_{diel} = V_{scr} - (-V_{plate}) > 0$, if $|V_{plate}| > |V_{scr}|$. But this procedure was also unsuccessful. Future work could be a replace of DC corona discharge power supply, V_{disch}, with an RF (radio frequency) voltage source (V_{disch}, RF ~ 3 kV, f ~ 0.1 – 1 MHz), which may generate more free positive charge carriers (positive ions). Additionally, it would be more convenient to keep the corona discharge voltage (V_{disch}) constant during calibration, measurements, and analysis.

13

2.2   Other experimental equipment

Consideration of humidity and temperature

Other physical parameters that influence dielectric surface charging are ambient temperature and relative humidity (RH). Humidity is one of the most significant factors which influences the corona discharges, and it has been demonstrated that the discharge measurements are significantly affected by the relative humidity [25]. Thus, as can be seen in Figure 6, an acrylic box with top and both sides plexiglasses, attached by a wood frame has been used for humidty control. The acrylic box has a flexible front door to allow operator to set up different experiments. The front door has an arm port with oversized round shape so that the operator can operate comfortably and this assures that the humidity can be controlled appropriately.
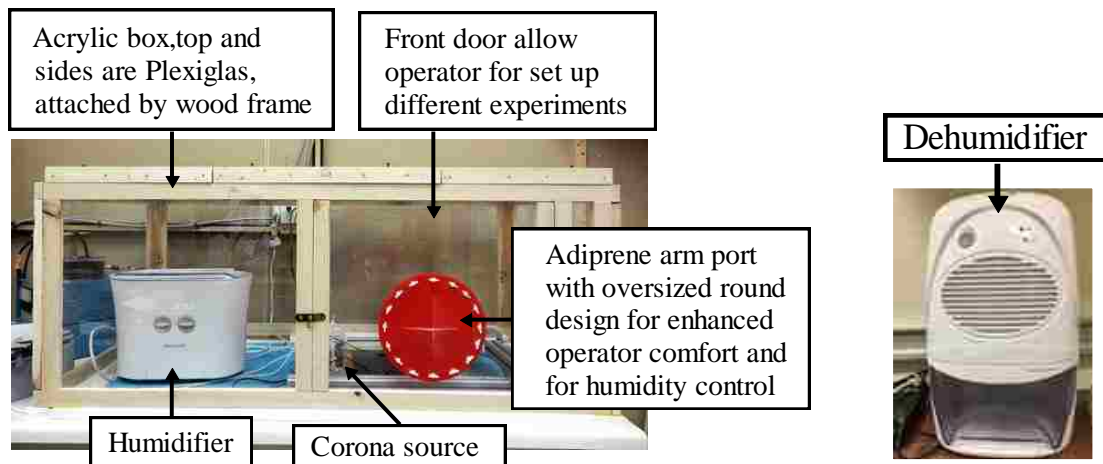
Figure 6: Left: Acrylic box with external wood frame for humidity control. Right: Dehumidifier for reducing humidity level.

A humidifier, model 2120K61 with adjustable output monitor manufactured by Honeywell has been used for this experiment (labeled 'Humidifier' in Figure 6 (Left)). This can raise RH up to 85% and covers areas up to 4,500 cu. ft. [26]. Additionally, A

14

powerful mid-size thermoelectric dehumidifier (model IVAGDM36, rate-16oz/24h at 86F, 80% RH), manufactured by Ivation has been used as shown in Figure 6 (Right). This can remove up to 20oz. of water per day, and can reduce the level of the humidity in the air of the acrylic box. This dehumidifier, with a removable water tank with a capacity of 53 ounces, is sufficient for spaces up to 2,200 cubic feet [27].

Electric field meter

A number of devices are now available for non-contact surface voltage or E-field strength measurement. In this work, a non-contact electric field meter, model M282, manufactured by Monroe electronics has been used for all experiments as shown in Figure 7.
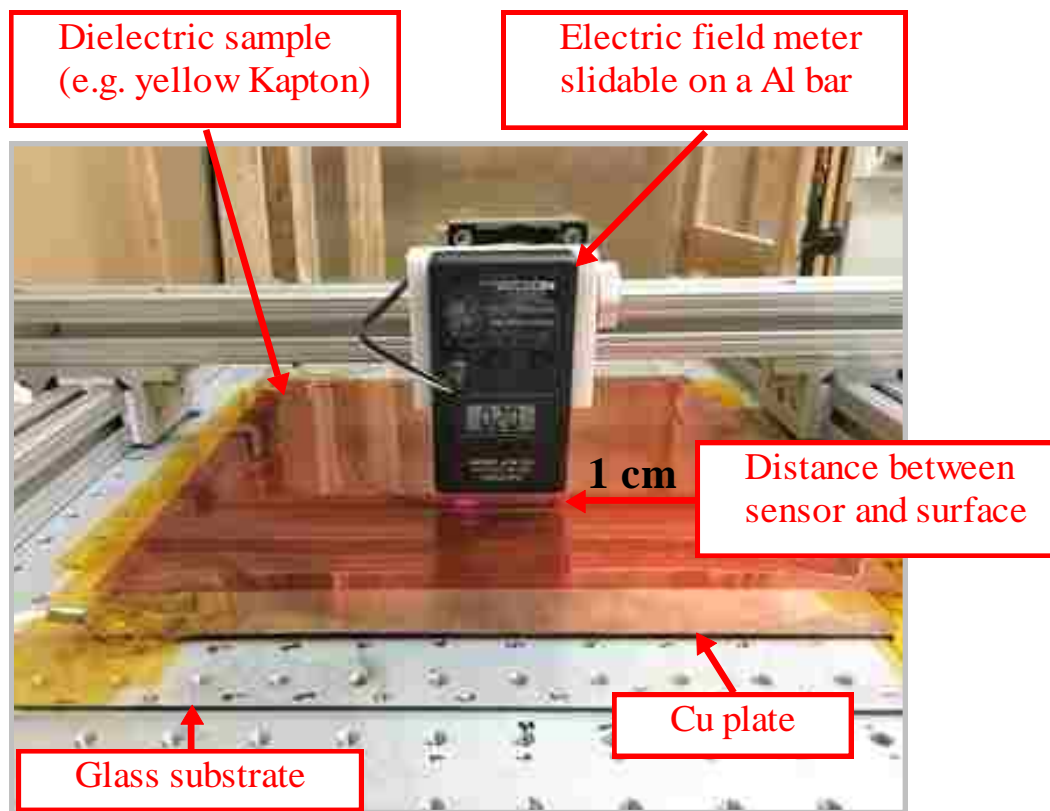
Figure 7: Configuration of electric field meter, model M282 manufactured by Monroe.

The input impedance of the non-contact field meter must be much higher than the surface to be measured [28]. The electric field meter is mounted on an aluminum bar which allows motion of the sensor in x-, y-, and, z-direction. This meter has a range finder LED beam, and can read up to +/-20 kV when the instrument is exactly 1 cm away from the target (labeled 'Distance between sensor and surface' in Figure 7). Following the manufacturer's instructions, the appropriate spacing between the sensor plate of the field meter and the tested surface has been maintained to get reliable measurements. In addition, the meter was grounded properly as specified by the manufacturer.

2.3 Dielectric materials for surface charging

Six dielectric materials have been tested under an ambient laboratory temperature and humidity conditions (*cf*. in Figure 8). The sample materials were black Kapton [29], semi-black Kapton [30], yellow/amber Kapton [31], Lexan [32], white Delrin [33] and red Adiprene [34].

Figure 8: Dielectric samples tested.

The size and geometrical configuration of the test materials were determined based on the availability in the market. The test dielectric samples were typically ~ 12 in. × 12 in. (30.5 cm × 30.5 cm). Table 3 gives a detailed description of various dielectric samples under test.

16

Table 3: Detail configuration of tested sample materials

Material	Thickness	Area ($in. \times in.$)
Black Kapton (Kapton B Polymide)	0.254 mm	$\approx 11.5 \times 13$
Semi-black Kapton	0.127 mm	$\approx 8.5 \times 11$
Yellow/amber Kapton	0.127 mm	$\approx 12 \times 12$
Lexan (Transparent polycarbonate Sheet, XL102UV)	2mm	$\approx 12 \times 12$
White Delrin (Acetal Homopolymer)	3mm	$\approx 11.5 \times 12$
Red Adiprene (Urethane Elastomer, unknown type)	2mm	$\approx 12 \times 12$

All materials were cleaned with methanol and allowed to dry before each test. The sample sheet was laid on the Cu plate (see details above), and the corona source was passed slowly twice without contact over the sample while both applied voltages (V_{disch} = –3 kV, $V_{scr} \approx$ –1 kV to –15 kV) remained constant. A much as possible, testing of of sample was made consistent by a systematic and repetitive experimental approach, with an identical temperature and humidity. Note that in order to get reliable measurements, an identical exposure time was maintained for each dielectric during the corona charging process. Additionally, the initial charge on any dielectric material were neutralized by applying the opposite charge polarity (same charge magnitude) using the corona source, or by using the brush tool before each test.

2.4 Brush tool experiment for surface charge removal

A consistent and reliable brush tool method was performed to remove surface charge from the dielectric samples. A number of commercially available brushes were utilized in order to eliminate surface charge, after charging the test dielectrics (*cf*. in Figure 9). These brushes were provided by Francis Martinez of LANL, who used them in his M.S. thesis research. Among these three brushes, two are manufactured by Gordon Brush Mfg. Co. Inc, and both brushes (grounded Brush #1, and ungrounded Brush #2) are designed with a static dissipative handle, while the third brush (ungrounded, Brush#3) utilized an aluminum handle (manufacturer is unknown). Both brush #1 and #2 are considered "conductive", with a resistance of approximately 1 MΩ between the bristle end and brush handle.

Brush#1: Grounded, operated manually, material - Thunderon® bristle.

Brush#2: Ungrounded, operated manually, material-Thunderon® bristle

Brush#3: Ungrounded, operated manually, material - Nylon bristle

Figure 9: Brush tools for dielectric surface charge removal.

Each brush is passed manually one time (1x), two times (2x), or three times (3x) for few seconds (≤ 5 sec) over the sample in order to test the effectiveness of charge removal from the surface. The grounded brush#1 appeared more effective than brush#2, or brush#3, and thus, grounded brush#1 was utilized for all experiments reported in this thesis.

Table 4 gives a clear comparison of the three brushes used for the surface removal effectiveness from a dielectric.

Table 4: Brush tool configuration for surface charge removal by corona source.

Brush tool	Brush material	Configuration
Conductive with drain wire Brush#1	Static dissipative handle (Material-Thunderon® bristle)	Grounded (connected via a wire to Al plate), operated manually.
Conductive Brush#2	Static dissipative handle (Material-Thunderon® bristle)	Ungrounded, operated manually.
Static dissipative Brush#3	Static dissipative handle (Material-Nylon bristle)	Ungrounded, operated manually.

CHAPTER 3: ANALYSIS AND DISCUSSION OF RESULTS

A series of experiments were designed to measure the surface voltage (in terms of electric field strength) of each dielectric before and after using the brush tool.

3.1   Experiment 1: Uniform charging and discharging at -1 kV

It is difficult and impractical to collect data on each single point of the surface of the materials. Instead, measurements at a few randomly chosen points on the sample surface were made. This is a random sampling process and was used to assess uniform charging on the dielectric surface (*cf.* in Figure 10a).

Figure 10 shows the dielectric surface charging by the corona source in order to produce a uniformly charged and discharged surface. First, the sample (in this case-yellow Kapton) has been charged by the corona source (see details above) at -1 kV (*cf.* in Figure 10b). Second, after charging, the corona source was removed and the E-field was scanned by the E-field meter to record the field at nine randomly chosen positions (*cf.* in Figure 10c). After taking spatial measurements by the E-field meter, the grounded brush#1 was used manually to remove the surface charge (*cf.* in Figure 10d). As the brush approaches the charged dielectric, a crackling can be heard in the region of the brush hair which is closest to the surface of the dielectric.
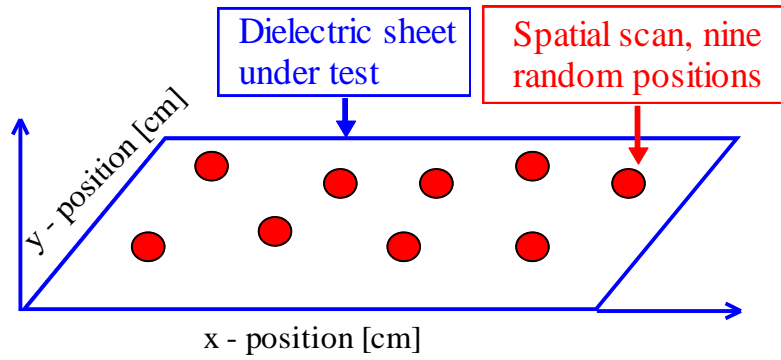
(a) Random measurement positions on dielectric
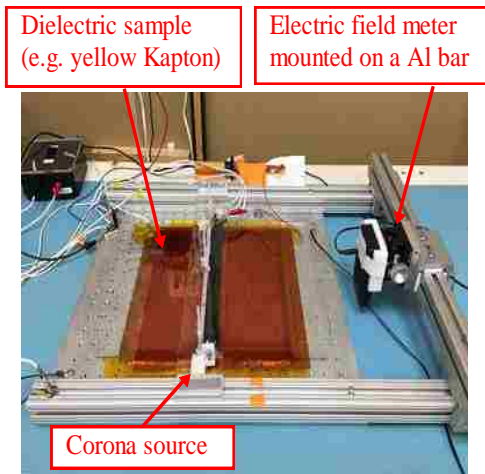
(b) Step 1 - Yellow Kapton charging by corona source
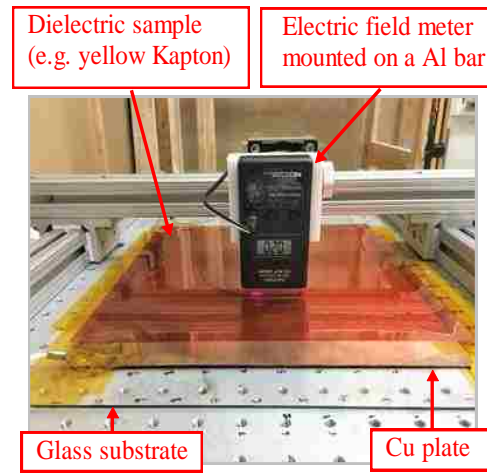
(c) Step 2 - Surface E-field measurements after corona charging
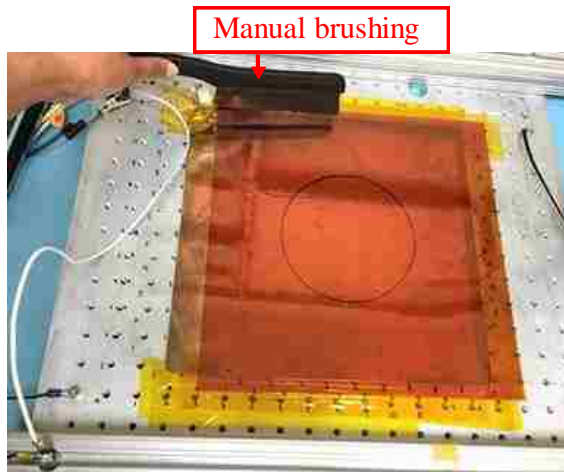
(d) Step 3 - Yellow Kapton discharging by manual brushing
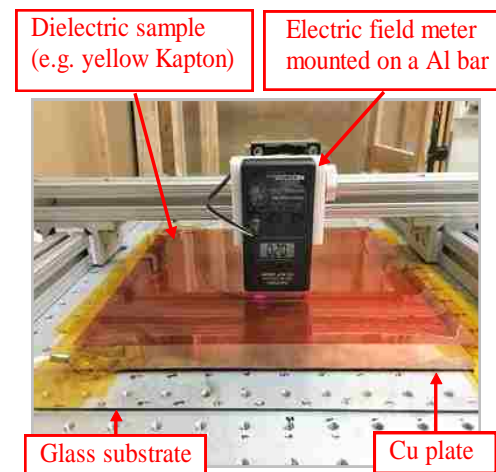
(d) Step 4 - Surface E-field measurements after brushing

Figure 10: Surface charging at -1kV and after brushing (e.g. yellow Kapton).

Finally, after one time (1x) brushing, the surface voltages were rerecorded by the E-field meter at the same positions where they scanned before brushing (*cf.* in Figure 10e). Typical results can be seen in Figure 11.
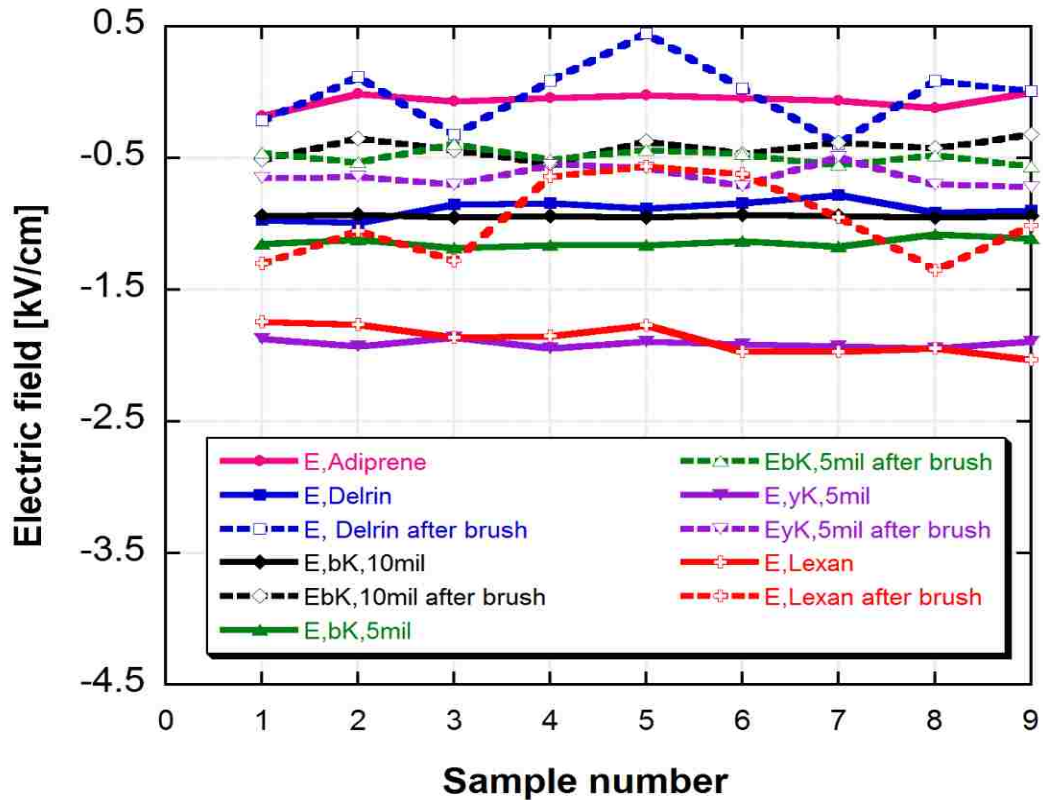
Figure 11: Surface E-field after corona charging at -1 kV and after brushing.

Figure 11 shows the spatial variation of different materials (i.e. black Kapton, semi-black Kapton, yellow Kapton, Lexan, white Delrin and red Adiprene) after charging at -1 kV and after brushing. As can be seen in Figure 11, black Kapton charged almost uniformly at $V_{scr} \approx$ -1 kV. Delrin and semi-black Kapton show to be relatively uniform, but Lexan and yellow Kapton are observed to charge to higher voltage (become more negative) than the charging voltage (corona source screen voltage). Adiprene didn't charge appreciably.

Several attempts using positive screen voltage, $V_{scr} \approx + 600$ V to +15 kV, were made. However, no reliable positive charging was obtained. After brushing, the grounded brush#1(one pass) removes approximately 50% of the initial surface charge from all dielectric materials except Lexan. Lexan shows a significant discharging nonuniformity (*cf.* Figure 11). That is, one pass brushing eliminates almost 75% of the surface charge at few points but only 50% of the charge at other points. We assume that surface charge, $Q_{surface} = C_{sample}V_{diel}$, where, C_{sample} = capacitance of dielectric sample which remains constant and V_{diel} = surface potential of dielectric sample. Thus, the surface charge removal is proportional to reduction of the surface potential, V_{diel} ($V_{diel} = E_{diel} \times 1$ cm). Subsequent brushings (2x, 3x) result in only small additional reductions.

3.2   Experiment 2: Uniform charging and discharging at -10 kV

However, subsequent brushings (1x, 2x, 3x) remove approximately 80-90% surface charge as can be seen in Figure 12.
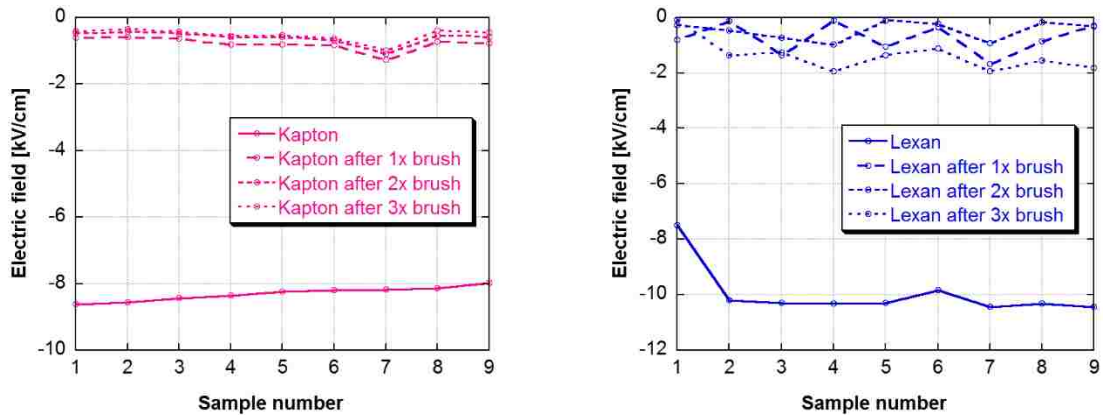
Figure 12: Surface E-field after charging (solid lines) by corona source at -10 kV and after brushing (dashed lines). Left: Black Kapton. Right: Lexan.

This shows a similar result to Figure 11 but at higher screen voltages, V_{scr} = -10 kV. Several attempts using different screen voltages at -1 kV, -3 kV, -6 kV, -10kV, -15kV, were made on all tested materials (i.e. black/semi-black/yellow Kapton, Delrin, Lexan). It was found that surface potential of some dielectrics discharged with time in complex ways at higher $V_{scr} \geq$ -2 kV (typically). Considering this phenomenon (discharging with time), only black Kapton and Lexan, which were relatively "well-behaved", were investigated to observe uniformity and brush removal effectiveness at -10 kV, as shown in Figure 12.

3.3   Experiment 3: Passive discharging vs. time measurements

By following the same steps of the corona charging process (see section 2.1), all dielectric samples were charged by passing the corona source over the sample for approximately 15-20 seconds. Immediately after the charge deposition on the dielectric surface, the corona source was removed and surface electric field measurements were taken versus time in a fixed position (typically near the middle of the surface).

For example, Figure 13 shows passive discharging versus time for yellow Kapton. First, yellow Kapton was placed on the Cu plate as shown in Figure 13 (Upper). Corona source voltages, V_{disch} = -3 kV (typically), V_{scr} = -10 kV (in this case) were applied to the corona source. The corona source passed twice over the yellow Kapton for approximately 15-20s. After that, the corona source was removed and the electric field meter was placed immediately over the yellow Kapton with 1cm spacing as can be seen in Figure 13 (lower). The surface electric field measurements were recorded at a fixed position [in this case (x, y) = (5.5, 7)], for 10 mins with 10-15s intervals.
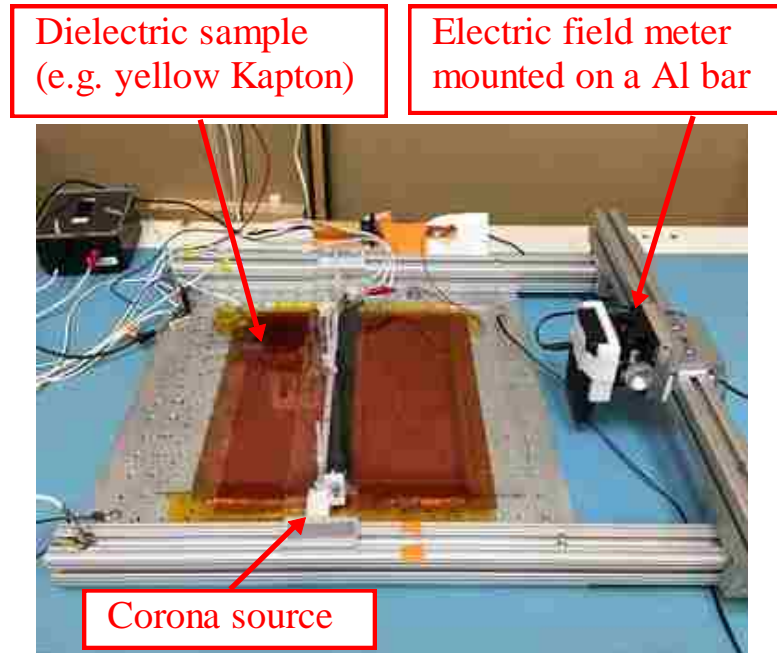
(a) Step 1: Surface charging by corona source (e.g. yellow Kapton).
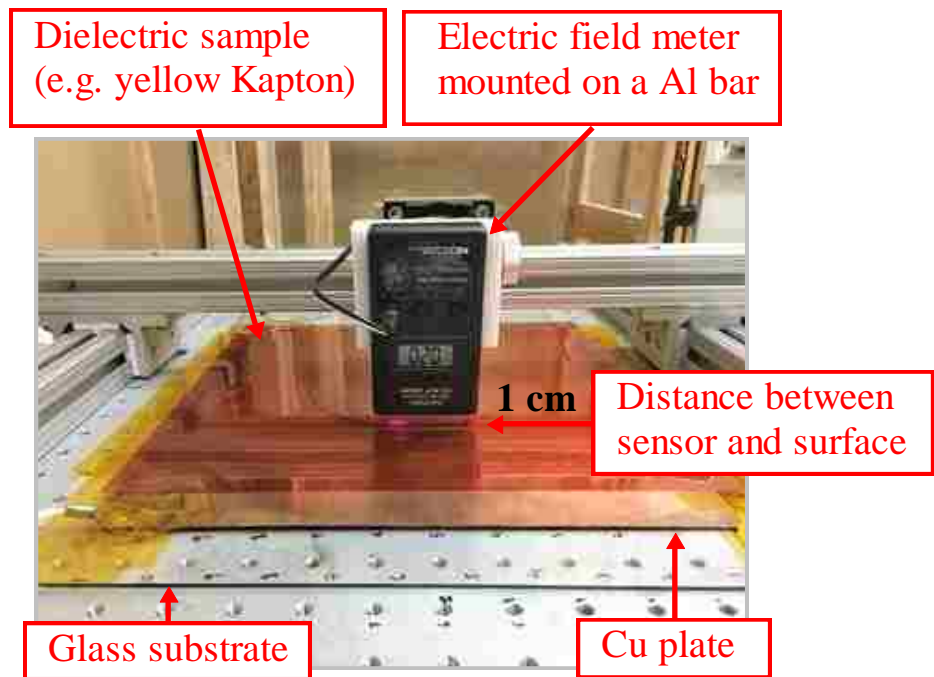
(b) Step 2: Surface E-field measurements with time at a fixed position.

Figure 13: E-field vs. time measurements by Monroe 282M E-field meter at a fixed position for 10 min with 10-15s intervals. Upper: Surface charging by corona source (e.g. yellow Kapton). Lower: Surface E-field measurements when corona source was turned off at t = 0.

Table 5 shows an example of the recorded data for yellow Kapton at -10 kV.

Table 5: Recorded values of surface electric field at 1 cm spacing by Monroe M282 electric field meter on yellow Kapton (surface was initially charged at $V_{scr} \sim -10$ kV and corona source was turned off at t = 0).

Time (min)	Electric field (kV/cm)
0:10	-9.05
0:20	-8.74
0:30	-8.56
0:45	-8.38
1:00	-8.29
1:15	-7.95
1:30	-7.75
1:45	-7.55
2:00	-7.41
2:30	-7.13
3:00	-6.89
3:30	-6.68
4:00	-6.51
5:00	-6.19
6:00	-5.96
7:00	-5.74
8:00	-5.54
9:00	-5.37
10:00	-5.21

For the next experiment, or for recharging the material for another screen voltage (V_{scr}), the negative charges on the top surface of the dielectric were removed by applying opposite polarity or by brushing the surface. The procedure described above for yellow Kapton was followed for other materials as well.

Figure 14: Measured surface electric field versus time for yellow Kapton at various charging voltages (i.e. -3 kV, -6 kV, -10 kV and -15 kV).

An example is shown in Figure 14. In this case, yellow Kapton was initially charged at applied voltages, V_{scr} = -3, -6, -10, -15 kV, and corona source was turned off at t = 0. As can be seen, the surface potentials decrease quickly from negative towards zero and the time responses are well fit by a single exponential decay $E = A - Be^{-t/\tau}$, where E is the surface E-field, A and B are constant values, and, t and τ are the time and time constant respectively.

Figure 15: Measured surface electric field versus time for semi-black Kapton at various charging voltages (i.e. -4 kV, -6 kV and -10 kV).
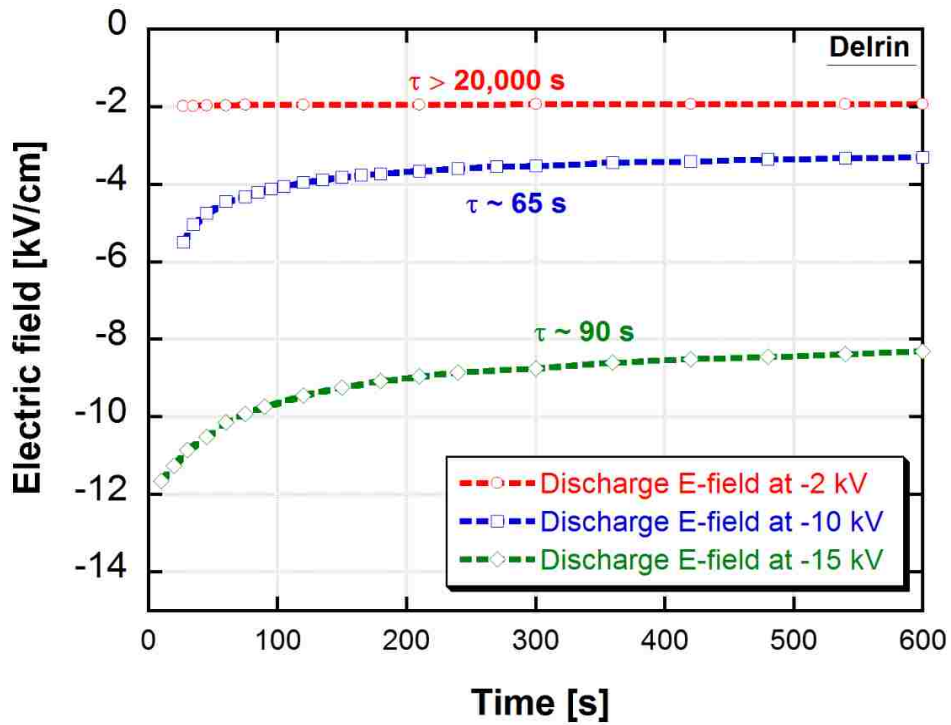
Figure 16 : Measured surface electric field versus time for Delrin at various charging voltages (i.e. -2kV, -10kV and -15kV).

28

Similar examples are shown in the following Figs (*cf*. in Figure 15 and Figure 16) for semi-black Kapton and Delrin respectively. Compared with yellow Kapton, Delrin and semi-black Kapton discharge slowly towards zero for cases of lower voltages ~ -2, -4 kV, and the data are well fit by a single exponential time constant, as indicated.
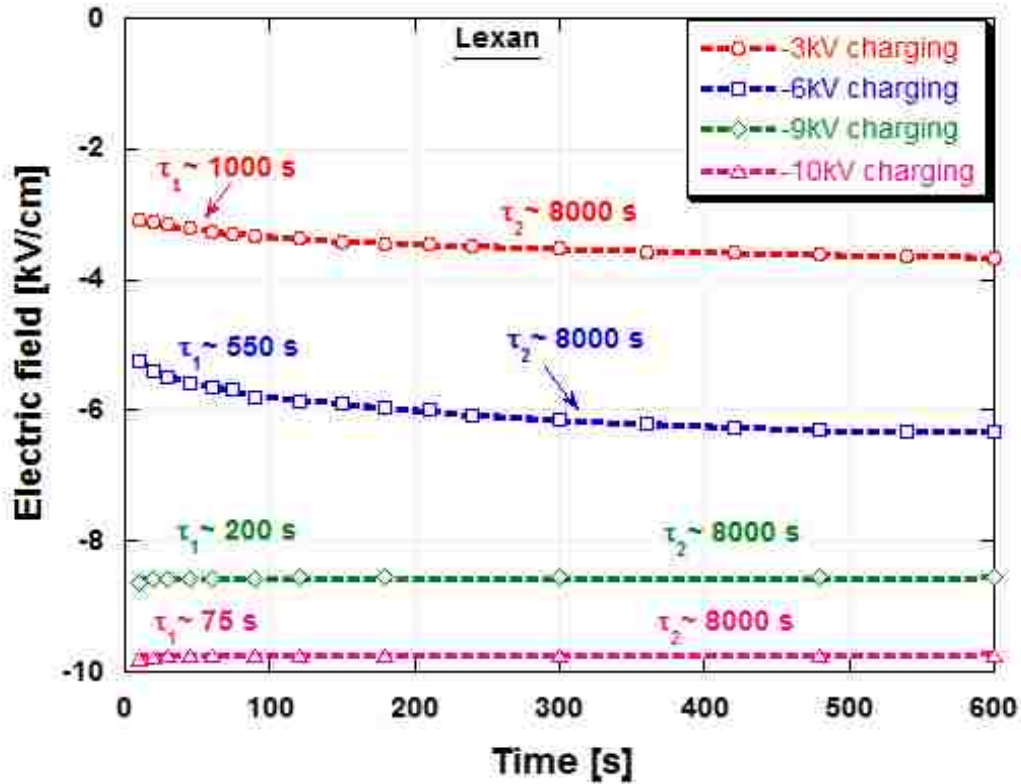
Figure 17: Measured surface electric field versus time for Lexan at various charging voltages (i.e. -3kV, -6kV, -9kV and -10kV)

In contrast to the above materials tested, Lexan exhibits much different relaxation behavior, as shown in Figure 17. Several features can be noted. First, the surface potential on Lexan increases in magnitude with time (becomes more negative) for cases of lower charging voltage ~ **-**3, **-**6 kV. Thus, Lexan appears to further charge itself on the surface. However, at higher charging voltages (**-**9, **-**10 kV), Lexan seems to discharge with time toward zero, as in the case of other materials such as Delrin, semi-black/black or yellow

29

Kapton. Secondly, while V_{diel} vs. time (relaxation) curves for other materials were well fit by a single exponential $\propto e^{-t/\tau}$, two exponential regions with different time constants (τ_1, τ_2) are required to reasonably fit the data of Lexan. As can be seen in Figure 17, the Lexan data are well fit at early times (t < 100 s, roughly) by one exponential $\propto e^{-t/\tau_1}$, and at late times (t > 100 s, roughly) $\propto e^{-t/\tau_2}$. Furthermore, the primary time constant (τ_1) varies with charging voltage (V_{scr}) but the secondary time constant (τ_2) is independent with V_{scr}. This seems to suggest that two different physical processes are at work in the relaxation of Lexan. In should be pointed that out these experiments were repeated several times, all with consistent results.
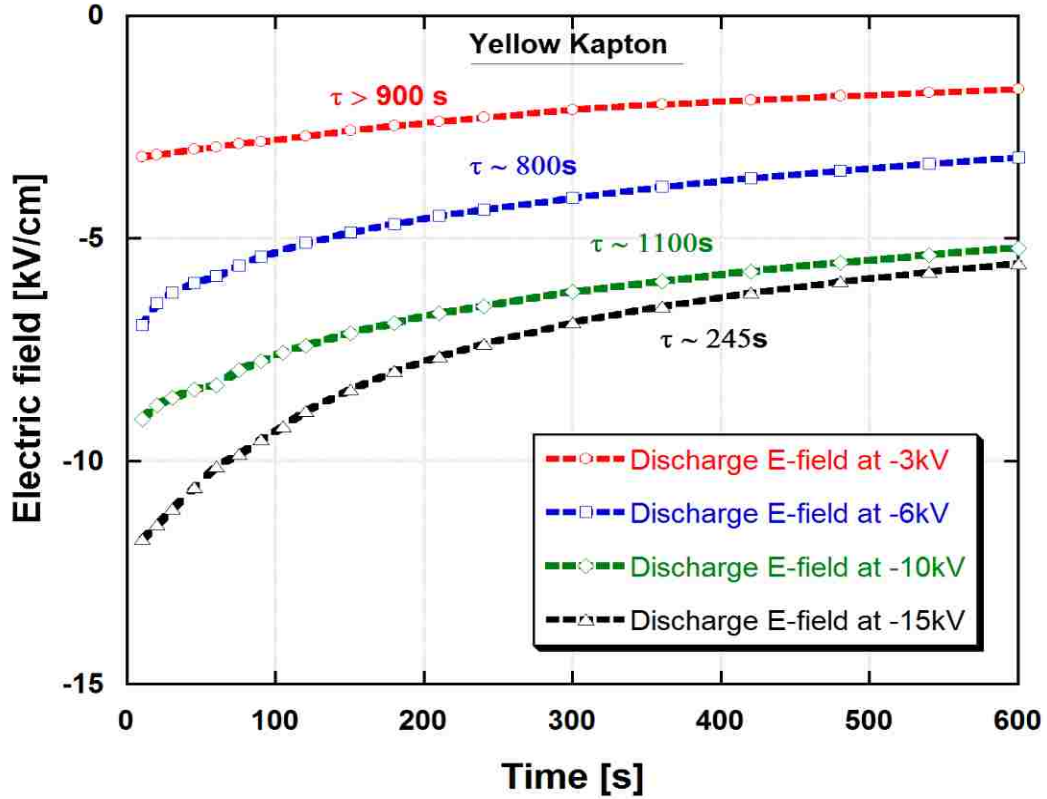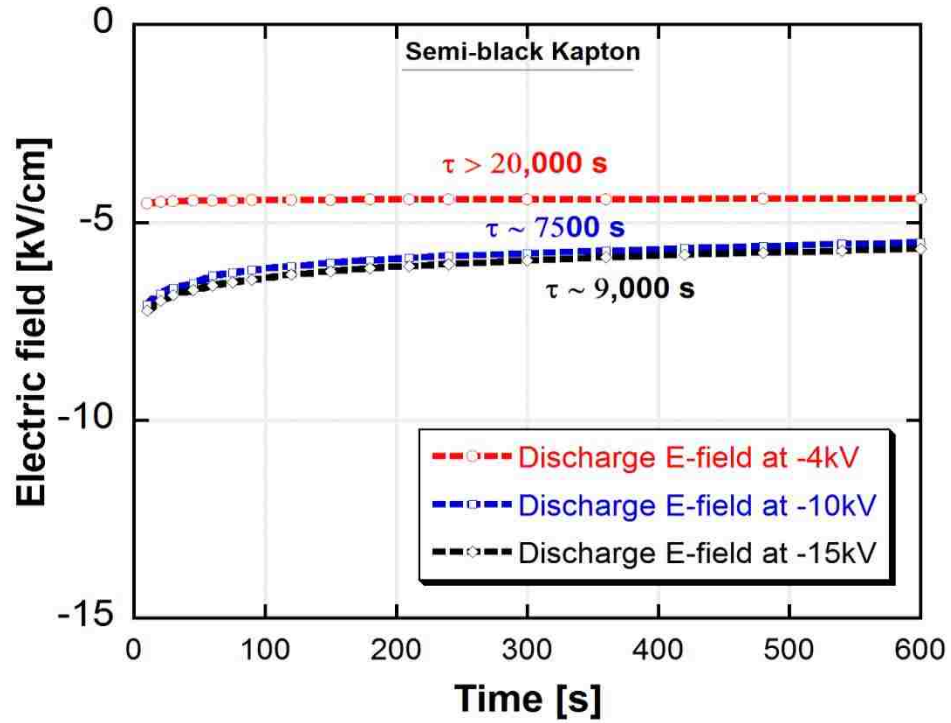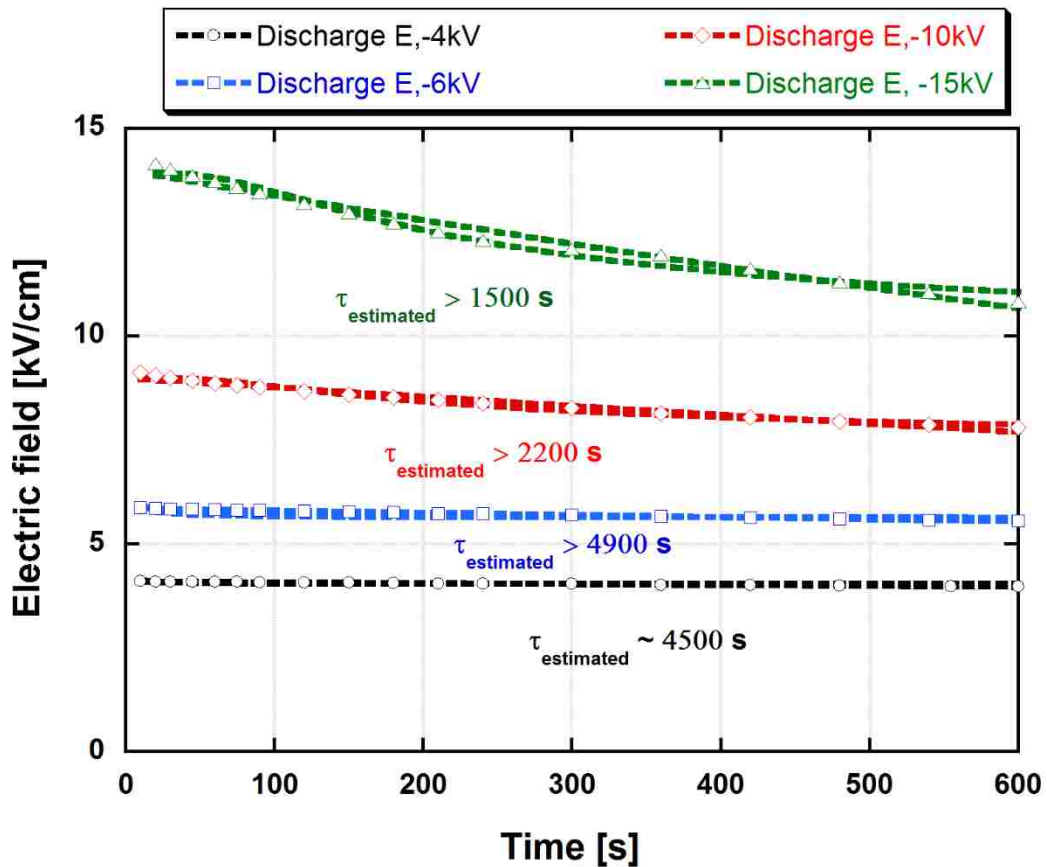

Figure 18: Measured surface electric field versus time for black Kapton at various charging voltages (i.e. -4 kV, -6 kV, -10 kV and -15 kV).

30

Another example can be seen for black Kapton at $V_{scr} \sim$ -3, -6, -10, -15 kV in Figure 18. In this case, the surface potentials were found to decrease from negative toward zero, and the time responses were well fit by a single exponential with time constant τ. As can be seen in Table 6, where time constants were calculated from the curve fit to the experimental data for the case of three cases of final voltage, $V_{diel}\,(\tau \to \infty)$: 1) an arbitrary asymptotic value was determined from the curve fit ($\tau_{arbitrary}$ in the table), 2) $V_{diel}\,(\tau \to \infty)$ = 0 (τ_0 in the table), and 3) for the final estimated value of $V_{diel}\,(\tau \to \infty)$ = -3.5 kV ($\tau_{estimated}$ in the table). The estimated final value was taken as $V_{diel}\,(\tau \to \infty)$ = -3.5 kV for black Kapton from observations after 4 hours from t = 0, when the corona source was turned off. Additionally, it was found that for charging voltages < -4 kV, time constants were too long to measure. As can be seen, the most accurate values of discharge time, τ, is given by $\tau_{estimated}$, these three values serve to bound τ due to experimental uncertainties.

Table 6: Time constant values for black Kapton at $V_{scr} \sim$ -4, -6, -10, -15 kV.

Charging voltage (V_{scr}) [kV]	Time constants [second]
-4	$\tau_0 > 1900$ $\tau_{arbitrary} \sim 950$ $\tau_{estimated} \sim 4500$
-6	$\tau_0 > 10{,}000$ $\tau_{arbitrary} \sim 950$ $\tau_{estimated} > 4900$
-10	$\tau_0 \sim 3400$ $\tau_{arbitrary} \sim 380$ $\tau_{estimated} > 2200$
-15	$\tau_0 \sim 2000$ $\tau_{arbitrary} \sim 333$ $\tau_{estimated} > 1500$

3.4   Experiment 4: Humidity variation of passive discharging

Discharging surface electric field measurements of the charged dielectric were also obtained in a closed acrylic box at a lower range of relative humidity of 16 – 22% and at a higher range of 27 – 37%, and effects of humidity were observed. All dielectric samples (except Adiprene) were charged followed by the same procedure described above. Examples for the case of $V_{scr} \approx$ - 10 kV are shown in Figure 19. As can be seen, higher humidity influences most of the materials to discharge more quickly. An exception is black Kapton, which seems to hold charge rather than discharge quickly.
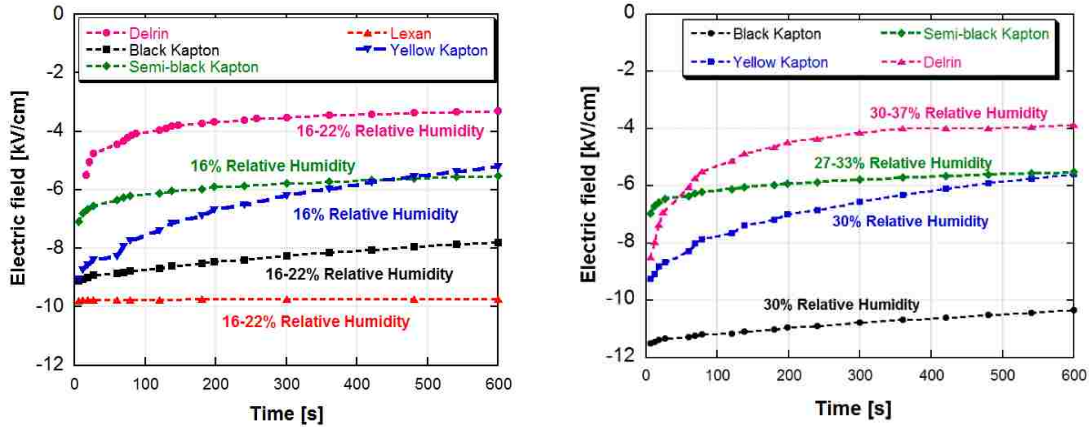
Figure 19: Measured surface electric field versus time for various materials at -10 kV. Left: At lower ambient relative humidity 16-22%. Right: At higher relative humidity 27-37%.

An attempt was made on yellow Kapton to observe the residual surface potentials after one min from t=0, as relative humidity was systematically varied. In this case, the charging voltage was -10 kV and the relative humidity was min. 16 % and max. 70%, with 10% variation. Results are shown in Figure 20. Another attempt was made with yellow Kapton for the cases of the lower range of relative humidity of 16 – 30%, and the higher range of 57 – 65%. In this case, yellow Kapton was charged at -3, -6 and -10 kV. The results can be seen in Figure 21.

32
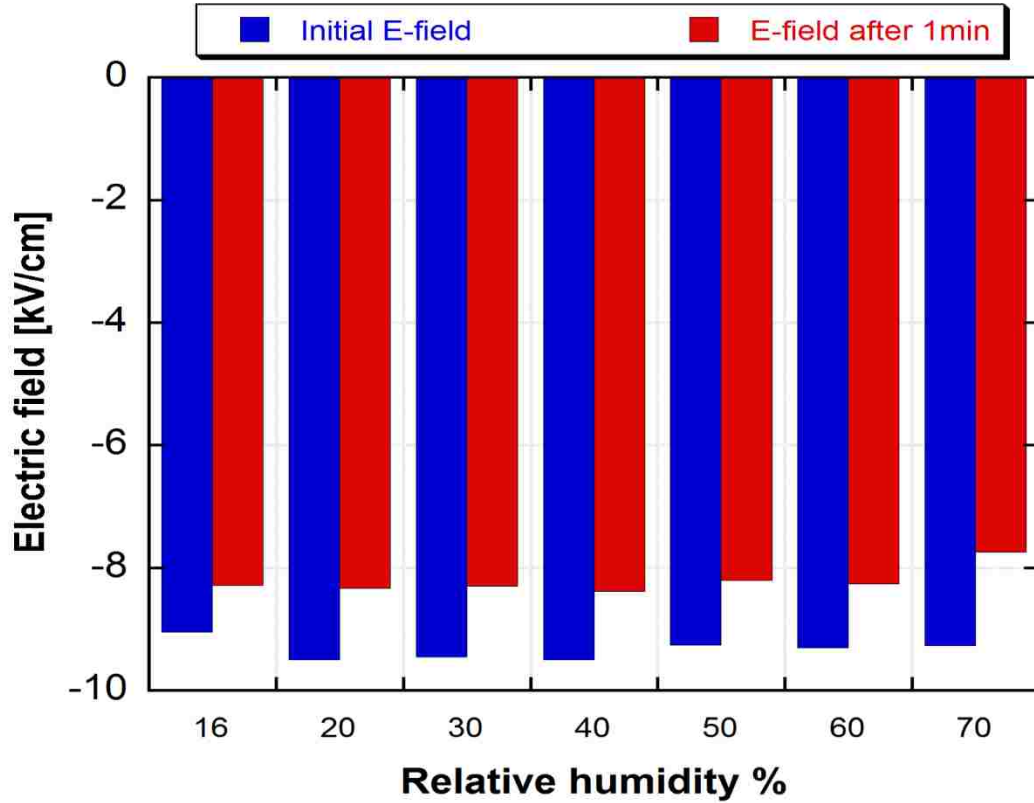
Figure 20: Initial and residual surface electric field measurements for yellow Kapton at -10 kV at relative humidity 16-70% with 10% variations.
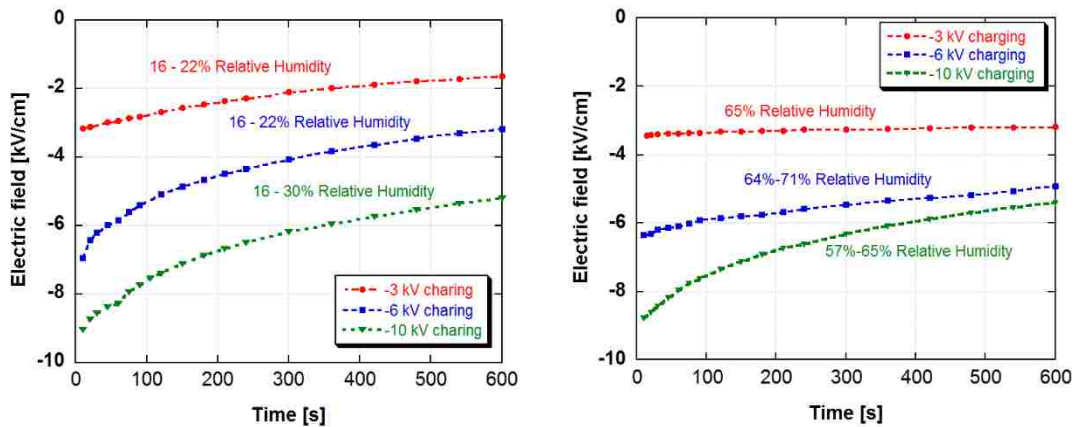
Figure 21: Measured surface electric field versus time for yellow Kapton at -3, -6, -10 kV. Left: At lower ambient relative humidity 16-30%. Right: At higher relative humidity 57-65%.

Table 7 and Table 8 show the initial surface voltages and the residual surface voltages after 10 minutes for the cases of lower range of relative humidity of 16 – 22% and the higher range of relative humidity of 27 – 37%. In this case, the surface samples were initially charged at V_{scr} = -10 kV. Immediately after charging, the corona source was turned off and electric field was recorded at t = 0 and t = 10 mins.

Table 7: Charge reduction (in terms of E-field strength, kV/cm) vs. time with RH 16-22%.

Material	Initial volts [kV]	Time [min]	Residual volts after 10 minutes, corona source was turned off at t = 0
Black Kapton	-9.11	10	-7.80
Semi-black Kapton	-7.09	10	-5.51
Yellow kapton	-9.05	10	-5.21
Lexan	-9.80	10	-9.74
Delrin	-5.50	10	-3.31
Red Adiprene	0	0	0

Table 8: Charge reduction (in terms of E-field strength, kV/cm) vs. time with RH 27-37%.

Material	Initial volts [kV]	Time [min]	Residual volts after 10 minutes, corona source was turned off at t = 0
Black Kapton	-11.50	10	-10.34
Semi-black Kapton	-6.96	10	-5.51
Yellow kapton	-9.25	10	-5.59
Lexan	-13.45	10	-12.85
Delrin	-8.50	10	-3.86

3.5 Experiment 5: Localized discharging at sample corner

The surface potential of the charged dielectric before and after using the brush tool in a localized area was also measured by brushing a relatively small area and making surface E-field measurements in the X- and Y- directions, as illustrated schematically in Figure 22. Localized brushing was investigated in order to understand the effects of localized discharging of a uniformly charged (approximately) dielectric surface. Localized discharging was mainly done by brushing grounded conductive brush #1 (see details above). The rest of the surface sample remained untouched.
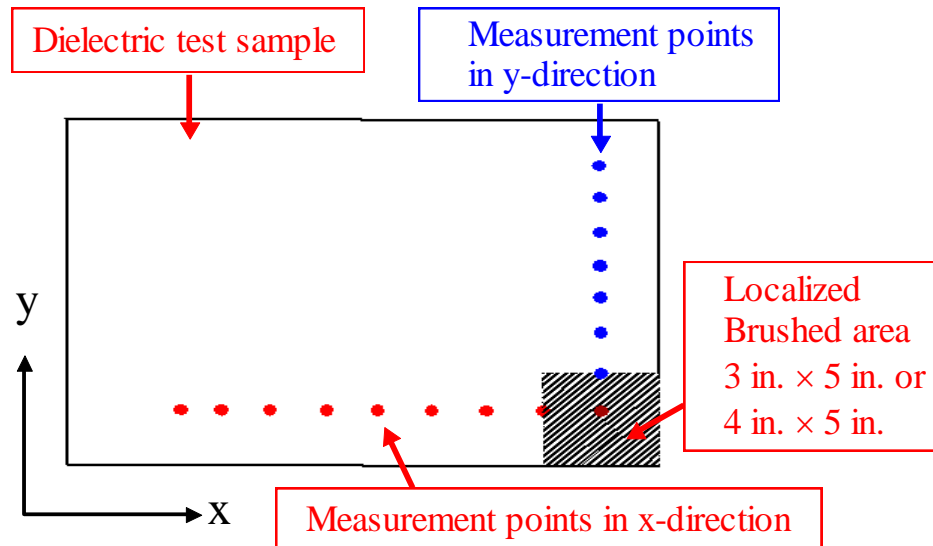
Figure 22 : Schematic of localized brush discharging at the corner of the sample.

However, first, a 'rectangular corner' area as indicated in Figure 22, (labeled 'localized brushed area'), of size 3 in. × 5 in. for Kapton and 4 in. × 5 in. for both Lexan and, Delrin, was selected for localized brushing. Second, once the dielectric sample was charged uniformly by the corona source as described in section 2.1, the E-field was scanned by the E-field meter in different y-positions (*cf.* Figure 22, 'Blue' circles). Third,

after one time brushing (by brush#1, see details above) over the 'rectangular corner' area, the E-field was rescanned in the same 'blue' circles in y-axis (data taken in the same points before brushing). Conversely, by following these same steps, E-field measurements were taken along the x-axis (*cf.* Figure 22, 'Red circles'). But before proceeding this step, the entire surface was brushed off by multiple brushings which removed the surface charge.
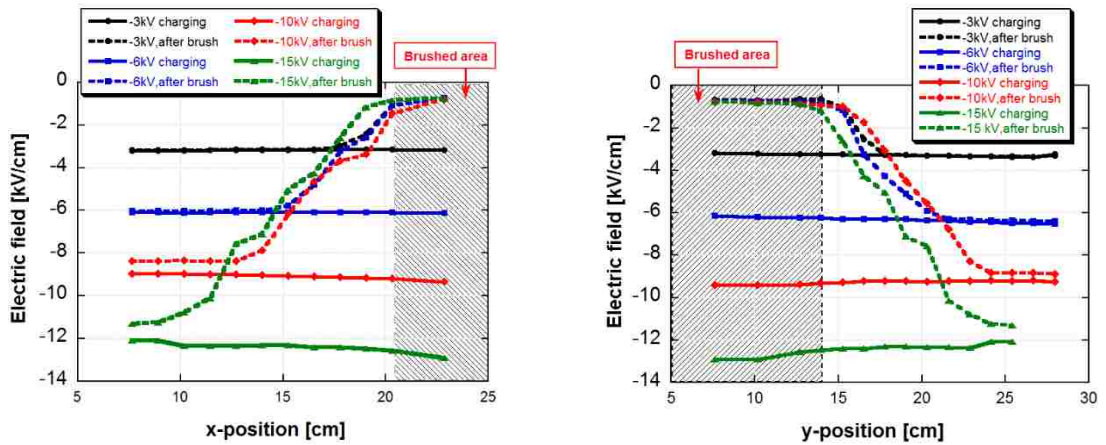
Figure 23: Kapton - Measured surface E-field in two orthogonal directions after charging at various source voltages, then localized brushing as indicated in Figure 22. Left: x-direction, Right: y-direction.

Figure 24: Kapton - Linear curve fits suggest nearly constant electric field gradients result outside the brushed area, as charge is redistributed across the surface over an area greater than the area brushed. Left: x-direction, Right: y-direction.

36

For example, Figure 23 shows the results of localized brushing for black Kapton in two different directions (x and y). These experiments were performed on the black Kapton at four different screen voltages, $V_{scr} \approx$ **-3 kV**, **-6 kV**, **-10 kV**, **-15 kV**. The solid lines and dashed lines represent charged (after charging and before brushing) and discharged (after brushing) surface potentials (V_{diel}) respectively. As can be seen, it appears that the surface charge inside and outside of the brushed area redistribute themselves so as to result in an approximately constant electric field gradient, ∇E between the brush discharged and fully charged area on dielectric, regardless of the initial charging voltage.

Linear curve fits on the region of electric field gradient give the values of gradient, between 0.538 and 1.00 kV/cm^2, with an average value of $\nabla E = 0.81$ kV/cm^2 as shown in Figure 24 in X- and Y- direction. It was found that there were no apparent differences in the values of the gradient, ∇E in x- and y-directions.

Another example can be seen in Figure 25, where Lexan also exhibits an approximately constant E-field gradient after localized brushing. As can be seen in Figure 26, Linear curve fits in the gradient regions give values of gradient, ∇E, between 0.74 and 0.87 kV/cm^2, with an average value of $\nabla E = 0.80$ kV/cm^2.
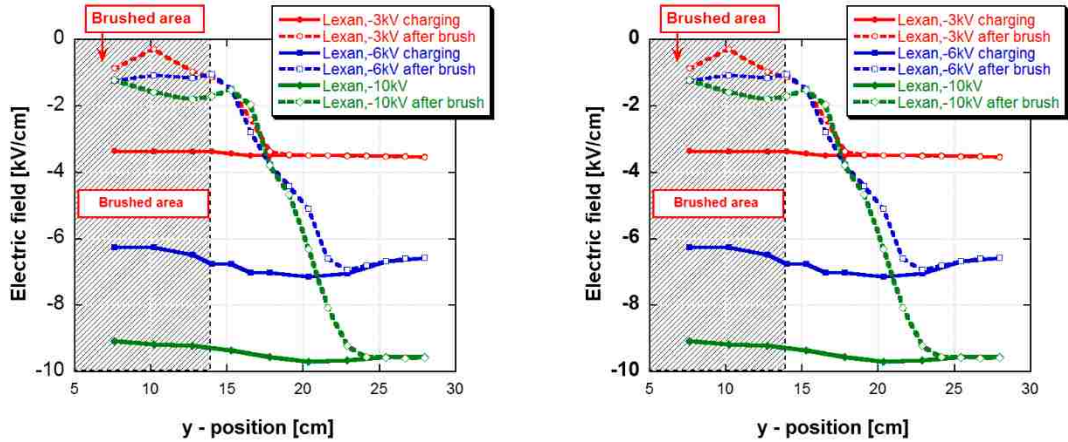
Figure 25: Lexan - Measured surface E-field in two orthogonal directions after charging at various source voltages, then localized brushing as indicated in Figure 22. Left: x-direction, Right: y-direction.

Figure 26: Lexan - Linear curve fits suggest nearly constant electric field gradients result outside the brushed area, as charge is redistributed across the surface over an area greater than the area brushed. Left: x-direction, Right: y-direction.

The following figs (*cf*. Figure 27, Figure 28, Figure 29) show the result of localized brushing for Delrin, yellow Kapton, and, semi-black Kapton respectively. These three materials were found to discharge quickly at charging voltages > -6 kV, so localized brushing was tested at charging voltages ~ (-3, -6, -10 kV). As can be seen, these three materials also exhibit an approximately constant E-field gradient after localized brushing.

38
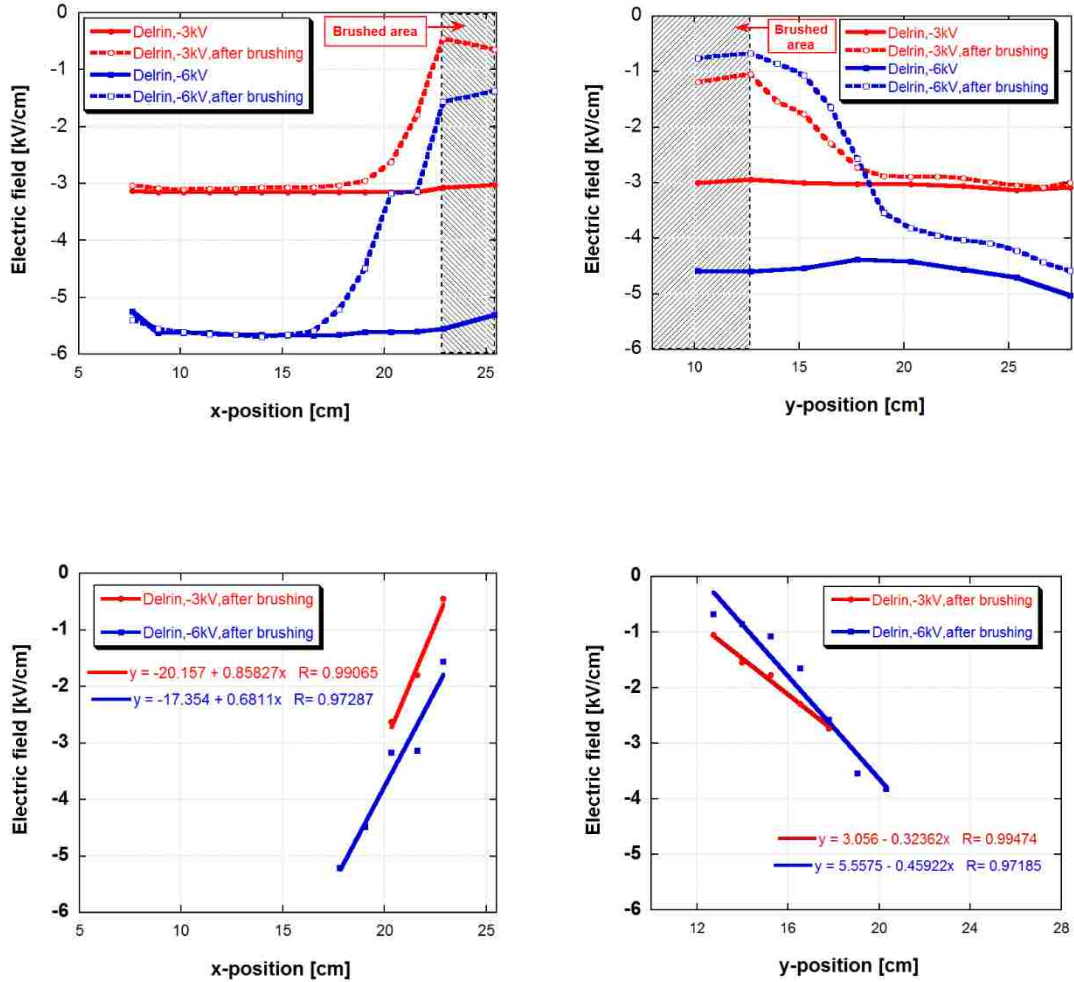
Figure 27: Delrin – Upper: **Measured surface E-field in two orthogonal directions after charging at (-3, -6 kV), then localized brushing as indicated in Figure 22. Left: x-direction, Right: y-direction. Lowe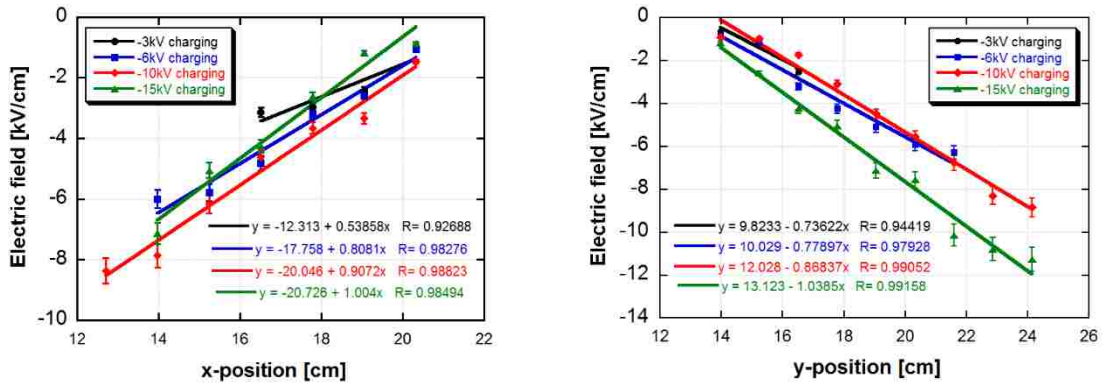r: Linear curve fits suggest nearly constant electric field gradients result outside the brushed area, as charge is redistributed across the surface over an area greater than the area brushed. Left: x-direction, Right: y-direction.**

For Delrin, linear curve fits give values of gradient, ∇E, between 0.33 and 0.86 kV/cm^2, with an average value of $\nabla E = 0.76$ kV/cm^2 (*cf.* in Figure 27). For yellow Kapton, values of gradient, $\nabla E = 0.81$ or -0.71 kV/cm^2 (*cf.* in Figure 28) and for Semi-black Kapton, values of gradient, $\nabla E = 1.08$ kV/cm^2 or -1.02 kV/cm^2 (*cf.* in Figure 29), were found.
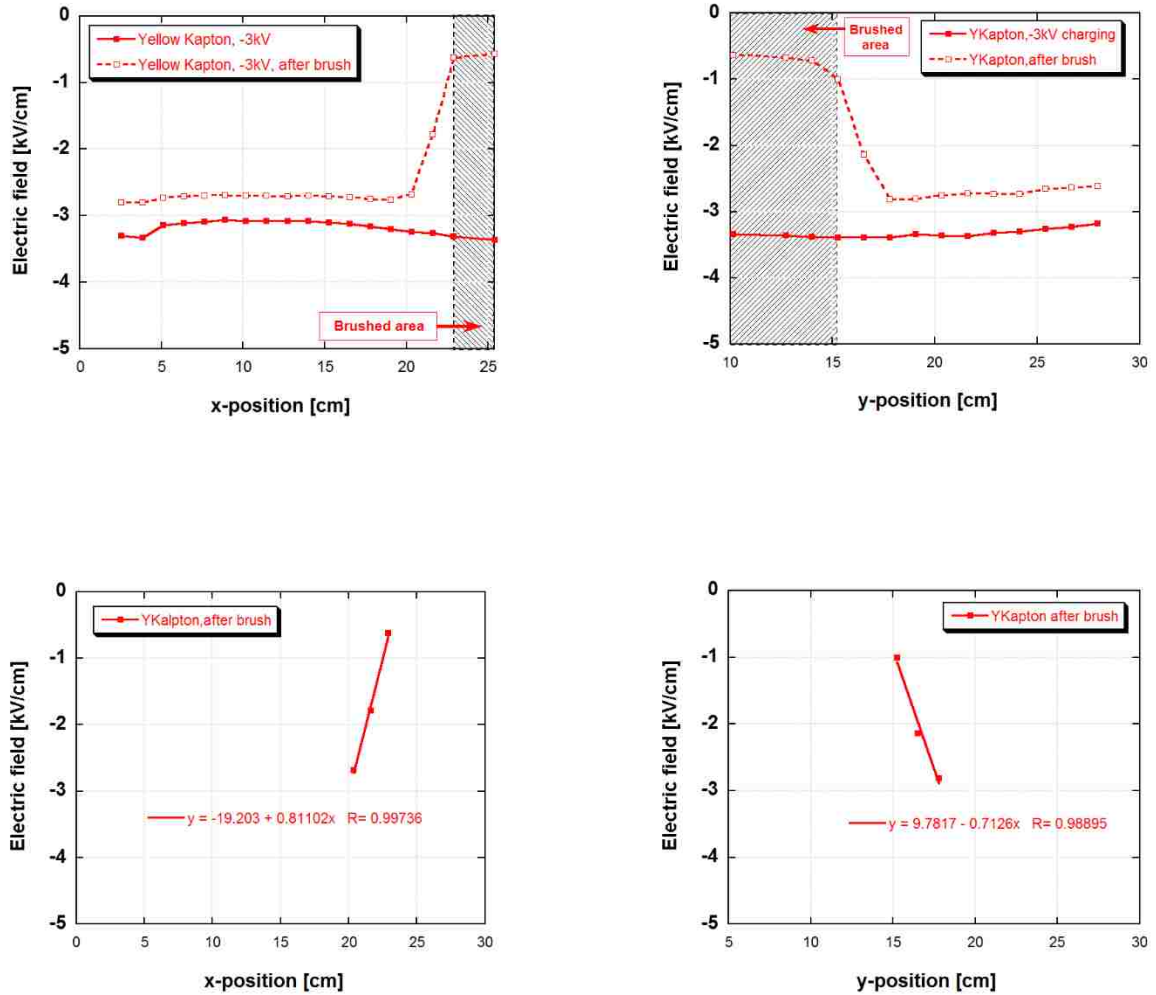
Figure 28: Yellow Kapton – Upper: Measured surface E-field in two orthogonal directions after charging at -3 kV, then localized brushing as indicated in Figure 22. Left: x-direction, Right: y-direction. Lower: Linear curve fits suggest nearly constant electric field gradients result outside the brushed area, as charge is redistributed across the surface over an area greater than the area brushed. Left: x-direction, Right: y-direction.
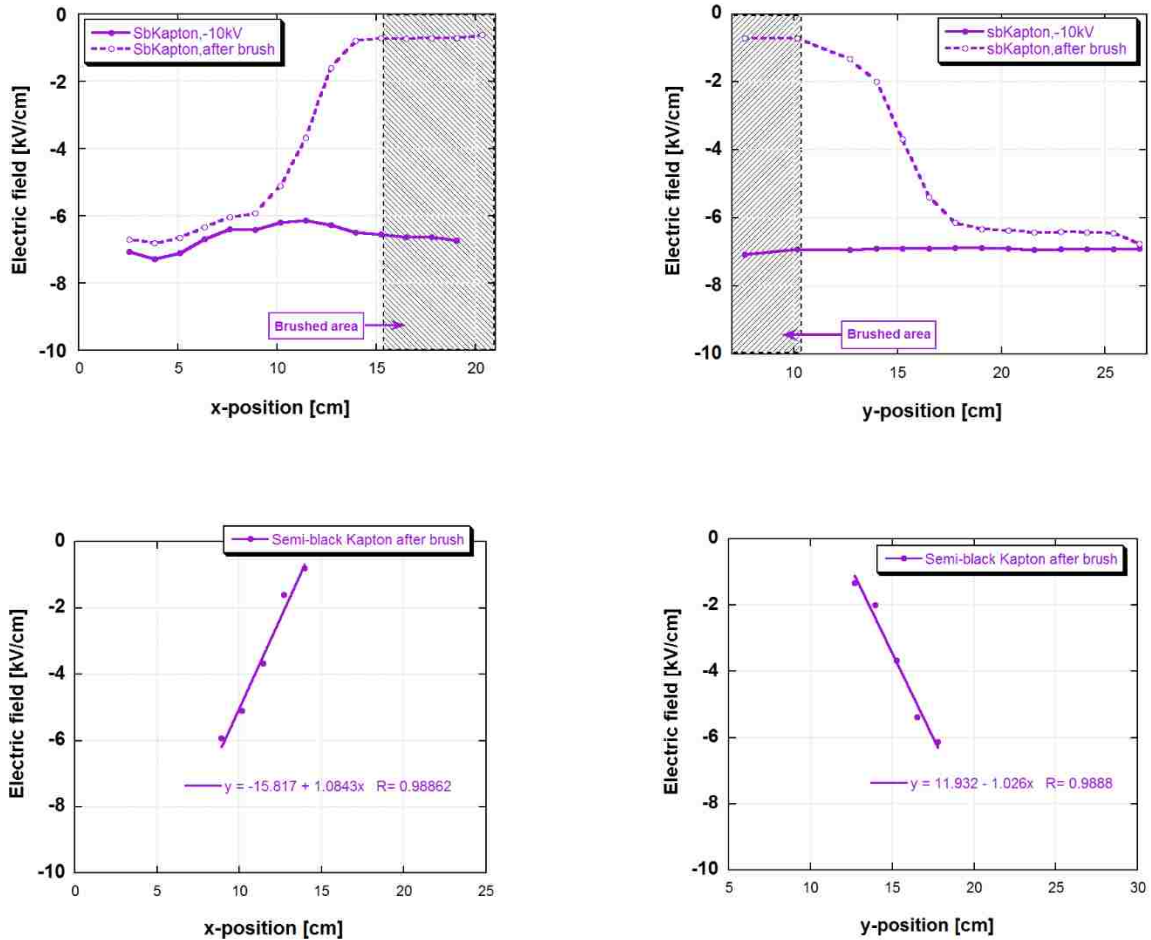
Figure 29: Semi-black Kapton - Upper: Measured surface E-field in two orthogonal directions after charging at -3 kV, then localized brushing as indicated in Figure 22. Left: x-direction, Right: y-direction. Lowe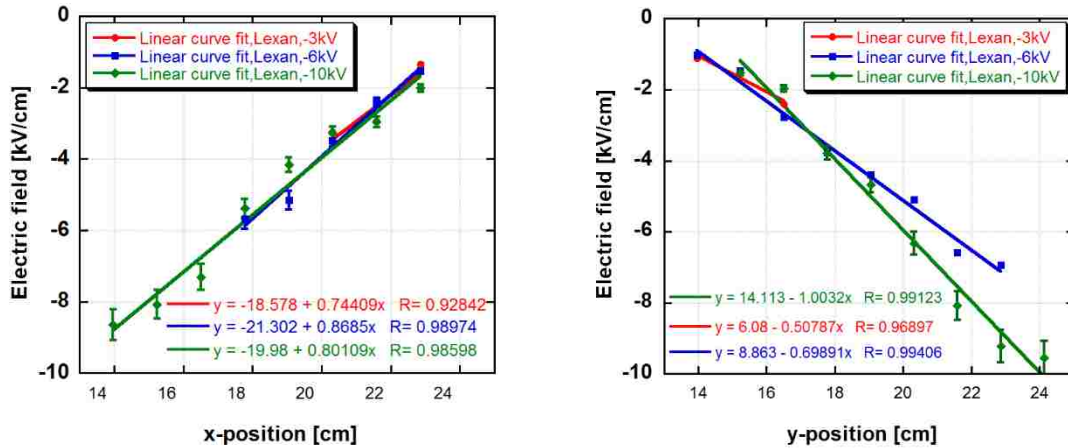r: Linear curve fits suggest nearly constant electric field gradients result outside the brushed area, as charge is redistributed across the surface over an area greater than the area brushed. Left: x-direction, Right: y-direction.

3.6 Experiment 6: Localized discharging at sample center

A slightly different approach to localized brushing was also performed by changing localized brushing area from the 'corner' to the 'center'. For investigating localized brushing at center, a 2.5 in. radius based circle was marked on the center of the sample. Note that since most materials are transparent (the exception is black Kapton), a circle was drawn underneath the sample in order to mark its boundaries.

41
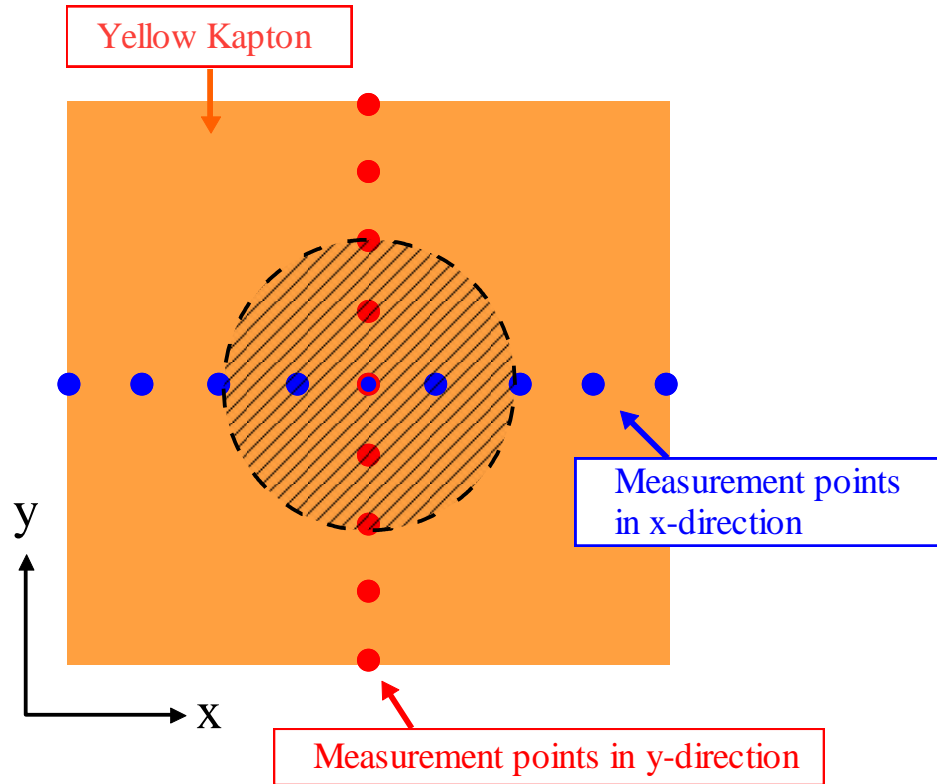
Figure 30: Schematic of experiments to study localized discharging by brushing in the sample center.

A schematic diagram of 'center localized brushing' for yellow Kapton is illustrated in Figure 30. The area of the yellow Kapton is a size of 12 in. × 12 in. (typically), therefore, the center point of the circle is (6, 6). The E-field was scanned by the E-field meter in the x- and y-directions before and after the brushing, as indicated in Figure 30. The entire experimental procedure of the central localized brushing remained unchanged from that described above for localized discharging at the corner (see section 3.5).

As already shown, yellow Kapton discharged rapidly with time at higher charging voltages > -3 kV. Thus, the effect of localized discharging at the center on yellow Kapton (~ uniformly charged surface) was observed at ~ -3 kV (*cf*. Figure 31) As can be seen, yellow Kapton exhibits an approximately constant E-field gradient after localized

brushing. Linear curve fits in the gradient regions give values of gradient, $\nabla E = 0.78$ kV/cm^2 in x-direction and between -0.47 to 0.83 kV/cm^2 in y-direction.
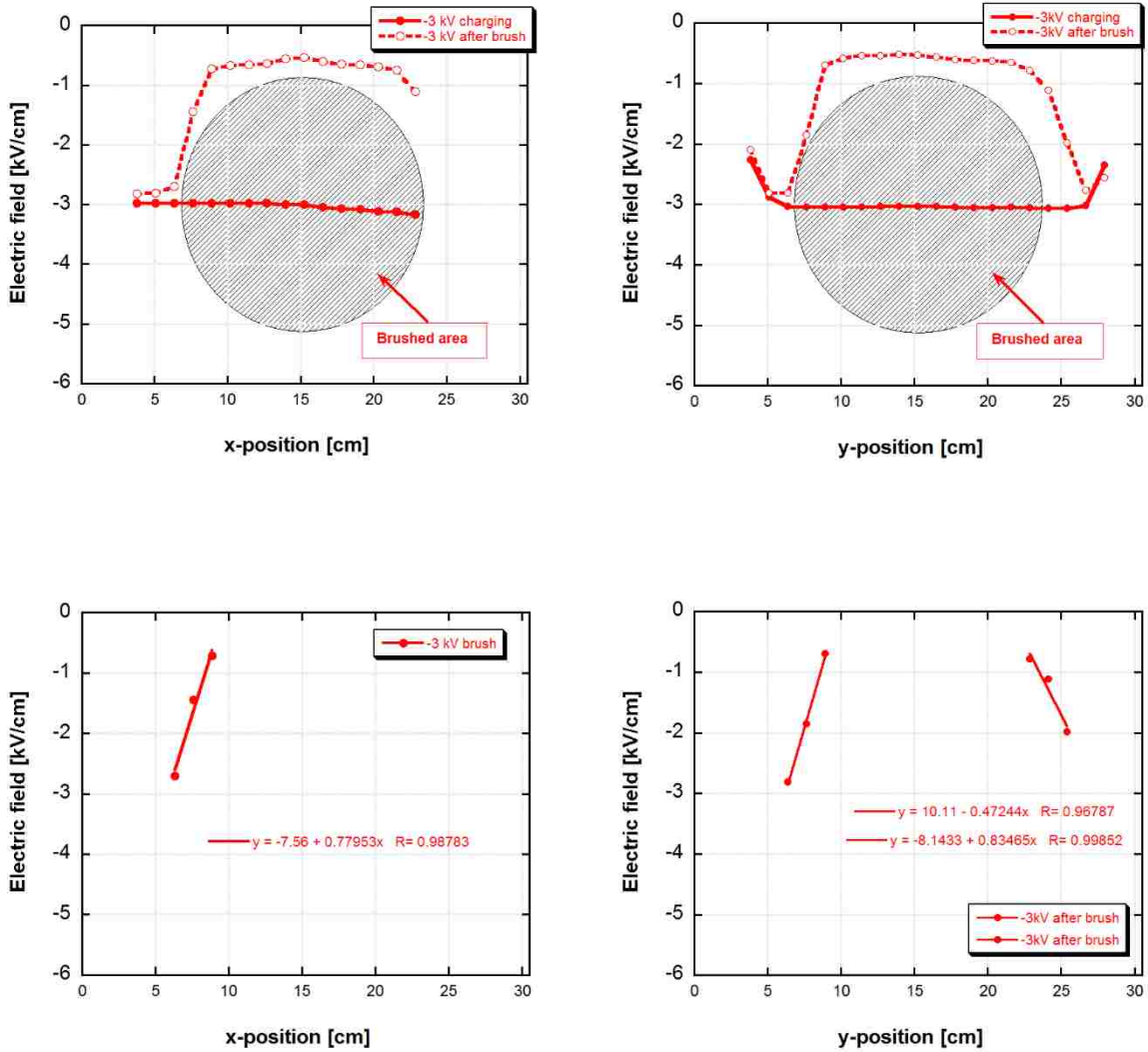
Figure 31: Upper - Localized E-field measurements via brushing by Monroe Electronics 282M field meter after charging of yellow Kapton dielectric by corona source. Lower - Linear curve fits suggest nearly constant electric field gradients result outside the brushed area, as charge is redistributed across the surface over an area greater than the area brushed. Left: x-direction, Right: y-direction.

## 3.7   Experiment 7: Brush tool effectiveness comparison

An experiment was conducted to observe the brush removal effectiveness among the three available brushes (see section 2.4). First, a sample was charged as usual by the corona source at $V_{scr} \sim$ -1 kV. After that, the corona source was removed and the E-field was scanned by the E-field meter at nine random positions (see details above). Once 9 random positions were recorded, brush#1 was passed over the sample for approximately 5 seconds (1x, 2x, 3x) softly and slowly by hand. The same procedure was then followed using brush#2 and brush#3, for comparison.

Figure 32 shows a comparison of the three brushes on black Kapton at corona source voltage, $V_{scr} \sim$ -1 kV. As can been seen in Figure 32(a), one time (1x) brushing of conductive brush#1 (grounded) reduces the surface potential > 50% from its original value. Subsequent brushing (2x, 3x) result in only small additional reductions. On the other hand, ungrounded brush#2 reduces surface potentials only a small amount at some points during successive brushings (2x, 3x) as shown in Figure 32(b). It can be seen in Figure 32(c), that brush#3 reduces surface voltages < 25% (probably > 25% at some points) but it seems less effective compared to the other two brushes (#1 and #2). Figure 32(d) demonstrates that brush#2 is more effective than brush#1, if it is grounded. As shown in Figure 32(b), brush#2 was ungrounded and did not remove surface charge appreciably, thus an attempt was made with ungrounded brush#2 by grounding it via a wire to the Al ground plate.
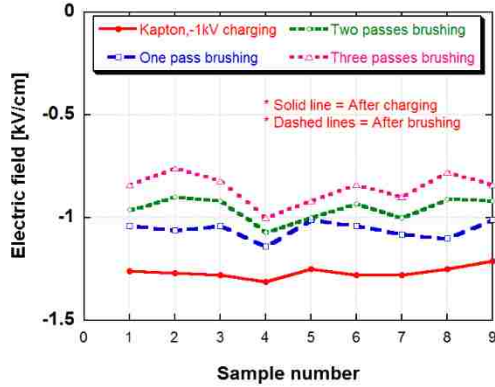
Figure 32 (a) – **Brush#1**: *Conductive grounded* with static dissipative handle, Thunderon® bristle material.
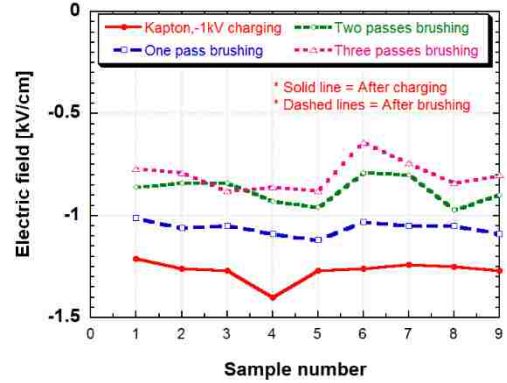
Figure 32 (b) – **Brush#2**: *Conductive ungrounded* with static dissipative handle, Thunderon® bristle material.
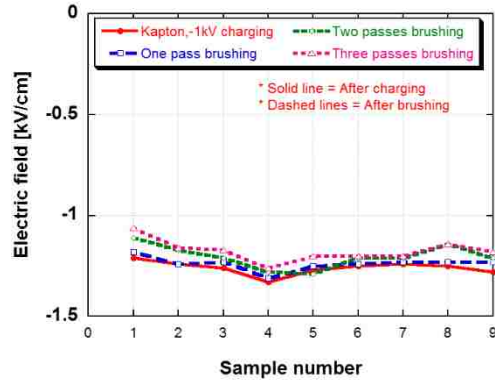
Figure 32 (c) – **Brush#3**: *Static dissipative ungrounded*, nylon bristle material.
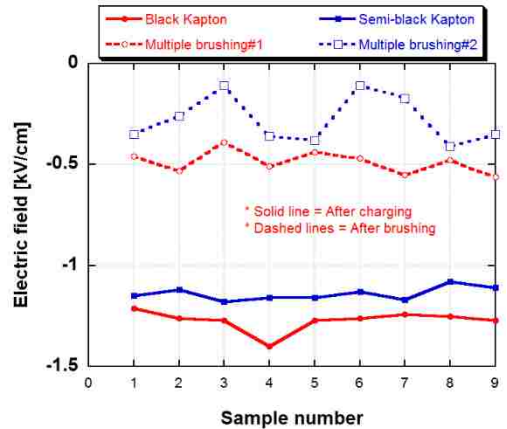
Figure 32 (d) – Comparison of **Brush#1** and **Brush#2** on Kapton. Both are *grounded.*

Figure 32: Electric field measurements by Monroe 282M E-field meter at 9 random sample points with threee different brushes at -1kV after charging by corona source (solid lines) and after brushing 1x (dashed lines).

3.8   Experiment 8: Influence of surface resistivity

A limited number of experiments were conducted on a systematic basis to explore if there is any correlation between the surface resistivity and charging/discharging behavior of the sample. This experiment was conducted in both the normal laboratory (open)

45

environment and in an acrylic box with a relative humidity of min. 16% and max. 71%.

As noted by Owen, on a surface, the resistance decreases in proportion to width, w, but increases proportionally with length, l [35]. Thus, surface resistance, $R = {kl}/{w}$, where, k is a proportionally constant. Now, if the geometry of a surface of a material is square, where $w = l$, the resistance of that surface would be equal to the proportionality constant value of k [35]. However, in this situation, the measurement of surface resistance with respect to the constant value of k (which is square) is called surface resistivity, ρ_s and the unit says ohms per square.
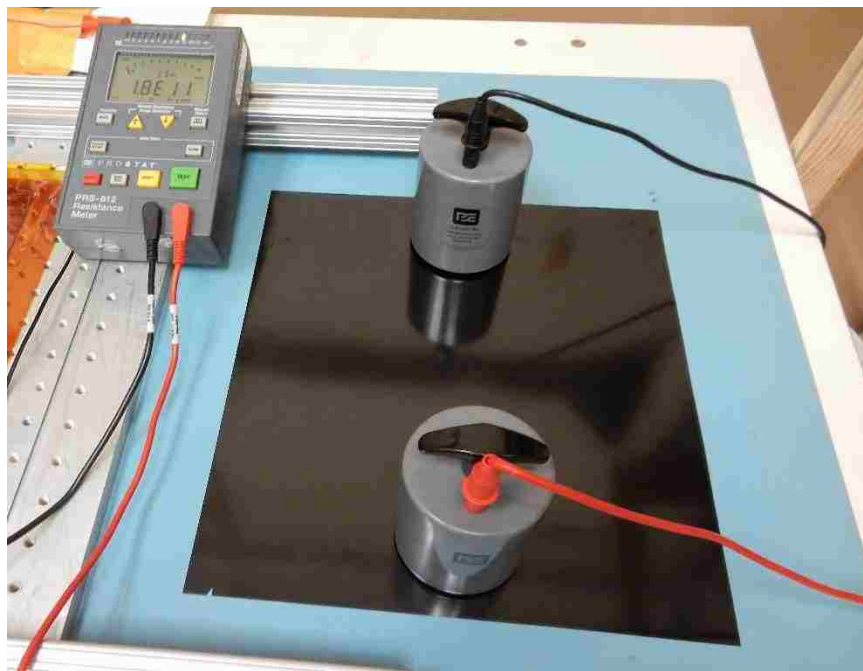
Figure 33: Measurements of surface resistance by PRS-812 test kits.

Surface resistivity has been measured by the PRS-812 resistance meter manufactured by Prostat as shown in Figure 33. The meter was provided by LANL for this project. The PRS-812 resistance meter is designed to measure resistance characteristics (dielectric

surface can also be measured) for ESD control per the American National Standards Institute (ANSI) standards [36]. In addition, for obtaining surface resistivity accurately, some preliminary steps (i.e. sample preparation, geometry of a sample, electrode configuration, humidity, temperature, etc.) have also been considered.

As per the PRS-812 manual, the meter has two 5 pound electrodes which measure resistance from < 0.1 to 1.0×10^{12} ohms with a measurement accuracy of $\pm 5\%$. As per ANSI standards, the electrodes were cleaned by methanol before obtaining any measurements. In addition, surfaces of the samples were cleaned by methanol and dried before each experiment. Each sample was measured by the PRS-812 at least 5 times and the average of the measured values was taken. Figure 33 shows an example of surface resistance measurements for black Kapton. In can be seen that the measurements were reasonably consistent for each material. Categorization of materials by surface resistivity defined by the Department of Defense are as follows [DOD Handbook 263 (1980)].

Table 9: Categorization of materials by surface resistivity [37].

Categorization	Surface resistivity $(\Omega / square)$
Conductive	$\leq 10^5$
Static dissipative	$> 10^5$ to 10^9
Antistatic	$> 10^9$ to 10^{14}
Insulative	$> 10^{14}$

Table 10 shows the surface resistance of the tested materials, measured by the Prostat PRS-812 Resistance Meter, listed by ordering them according to increasing surface resistivity.

Table 10: Surface resistivity chart of sample materials measured at RH 16-22%.

Test materials	Surface resistivity [Ω/square]
Red Adiprene	8.32×10^{10}
Yellow Kapton	1.42×10^{11}
Semi-black Kapton	1.68×10^{11}
Black Kapton	2.0×10^{11}
Delrin	2.22×10^{13}
Lexan	1.023×10^{14}

As can be seen in Figure 34, no correlation was found between the tendency of a dielectric to charge and its surface resistivity. Example data are shown in Figure 34, where it can be seen that yellow Kapton charges more than semi-black Kapton or Delrin, even though it (yellow Kapton) has lower resistivity. Even after 10 minutes, yellow Kapton still retains a significant amount of charge - more than Delrin. Similarly, semi-

black Kapton charges more than Delrin, and after 10 minutes, semi-black Kapton still holds more charge than Delrin. Further investigation is required to elucidate the complete behavior of the other dielectric materials.
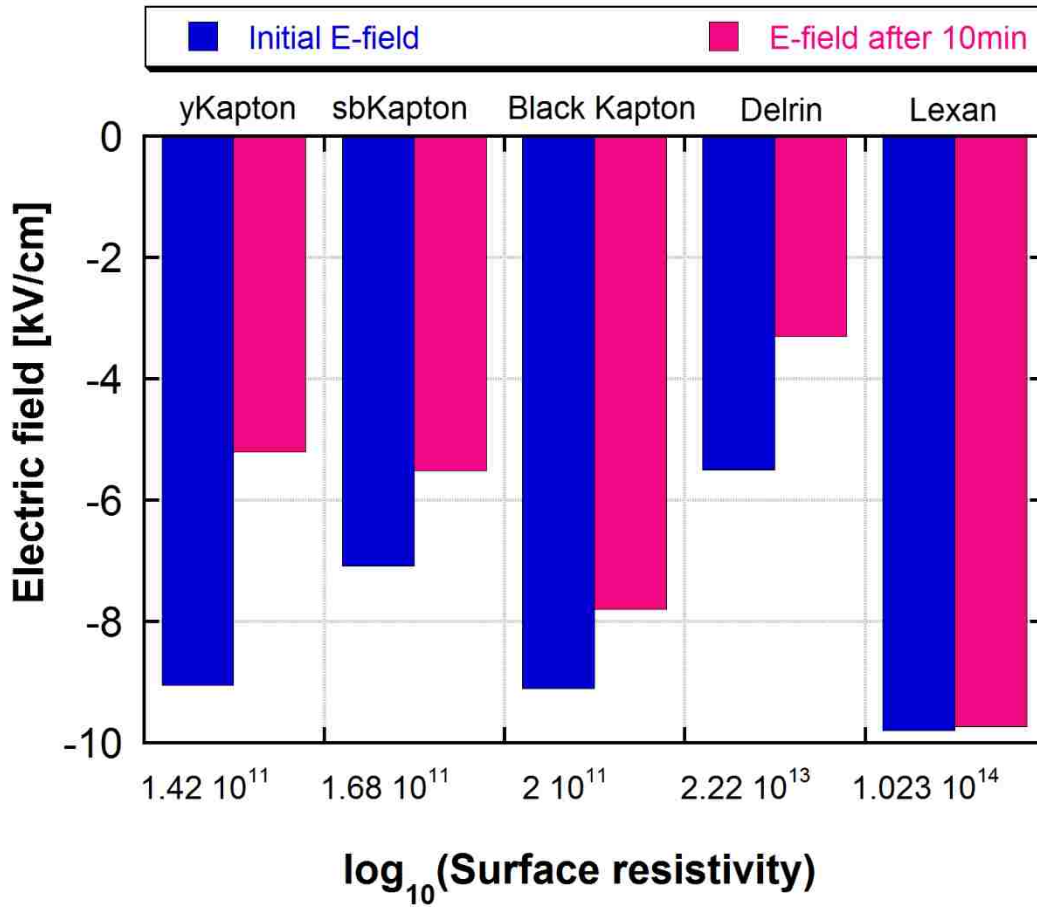
Figure 34: Relationship between surface resistivity and chargeability of all dielectric materials at -10 kV at lower ambient relative humidity, RH (16-22%).

CHAPTER 4: SURFACE CHARGE CALCULATION

The frequently stated relationship, $Q = CV$, is often used to analyze electrostatic discharge phenomena. Here Q, C, and V are the charge, capacitance, and voltage respectively. Once the capacitance, C_{sample}, of the dielectric can be determined, the surface charge can be computed since the surface voltage, V_{diel} is determined from the surface by E-field meter.

An electric field meter, model 282M, manufactured by Monroe Electronics (see details above in section 2.2), has been used to measure the surface voltage of the dielectric. The flat sensor plate of the E-field meter is placed above the charged dielectric surface at a fixed distance of 1 cm. Thus, the meter determines the electric field (E_{diel}) by measuring the surface voltage, where

$$E_{diel} = \frac{V_{diel}}{d} \qquad (1)$$

Note that the calibration distance of the E-electric field meter is 1cm for surface voltages up to $\pm$ 20 kV. For example, if the applied voltage is V_{diel} = -1 kV, and the distance is d = 1 cm, then the indicated electric field (E_{diel}) should be E_{diel} = -1 kV/cm.

4.1. Capacitance and surface charge density measurement

For better understanding and obtaining an accurate result, the capacitance (C_{sample}) of a tested material was both measured and calculated. It was found that, measured value is much lower than calculated value. Probably, there is an air gap between the bottom surface and Al plate. Thus, two capacitances (C_{sample}, C_{air}) in series reduce the actual

50

capacitance of the dielectric. In addition, since C remains constant, therefore from Q = CV, it can be stated that V is a good proxy to reduce the surface charge. This indicates that the following procedure for the measurement of capacitance using a water ring is reliable. Based on this assumption, capacitances of other tested materials have been measured by the method indicated in the schematic diagram shown in Figure 35.
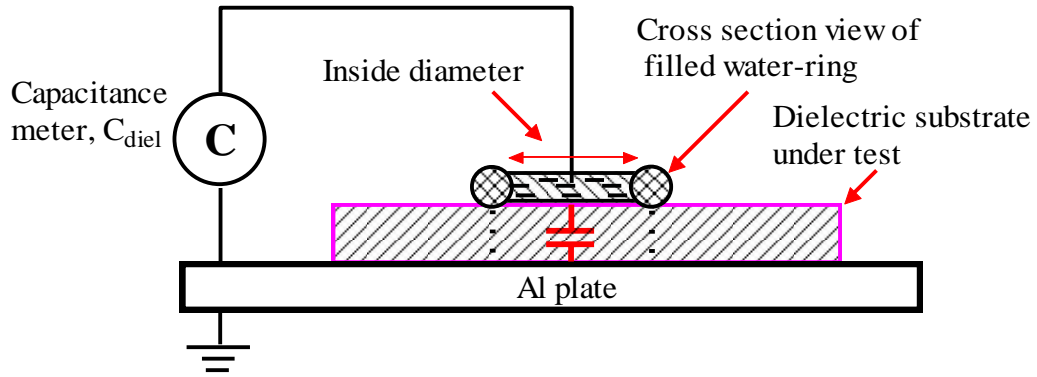
Figure 35: Schematic diagram for capacitance measurements.

However, the capacitance measurement is sensitive to a number of effects, and the important element is the measurement probe. The probe needs to be a good contact with the dielectric sheet, which needs to cover the entire probe area to get accurate measurements. To achieve the required contact, a small circular ring, filled with water was placed on one side of the dielectric surface, with a grounded Al plate placed under the sample, as indicated in Figure 35. One probe of the capacitance meter contacts water of the ring on sample surface and the other side contacts the ground plate as shown in Figure 35. The theoretical capacitance formula will be for this measurement,

$$C_{sample} = \epsilon_{diel}\epsilon_0 \frac{A_{surface}}{l} \qquad (2)$$

C_{sample} = Capacitance in farads of the dielectric sample

51

ϵ_{diel} = Dielectric constant of the material

ϵ_0 = Permittivity of free space ($\epsilon_0 = 8.854\times10^{-12}\,F/m$)

$A_{surface}$ = Total surface area of the dielectric under test

l = Thickness of the dielectric under test

Hence, with accurate measurements of capacitance, C_{sample}, and, surface voltage, V_{diel} as described in above, the total surface charge, $Q_{surface}$ can be computed by the following equations,

$$Q_{surface} = C_{sample}\,V_{diel} \qquad (3)$$

$$Q_{surface} = C_{sample}\,E_{diel}\,d \qquad (4)$$

And the surface charge density is then given by

$$\sigma_{surface} = Q_{surface}/A_{surface} \qquad (5)$$

$$\sigma_{surface} = (C_{sample}/A_{surface})E_{diel}\,d \qquad (6)$$

Substituting equation (2) into equation (6) gives

$$\sigma_{surface} = \epsilon_{diel}\epsilon_0 E_{diel} \qquad (7)$$

For determination of charge distribution over dielectric surfaces, a quantitative interpretation of the electric field measurement is required, and here, the electric field strength depends upon the distance to the surface of the dielectric. It is difficult to generalize the electric field and charge calculation procedures because the analysis depends on the geometrical configuration [38].

Using the equations above, the capacitance of yellow Kapton has been compared with the measured capacitance. Now let's assume the following in order to determine the calculated capacitance value of the dielectric sheet of yellow Kapton:

Thickness of yellow Kapton under test, $l = 5mil = 0.0127cm$

Dielectric constant of the Kapton under test, $\epsilon_r = 3.5$ [Given by manufacturer [39]]

Surface area of the yellow dielectric, $A_{diel} = 12inch \times 12inch = 929.0304cm^2$

From equation (2)

$$C_{yKapton} = \epsilon_{diel}\epsilon_0 \frac{A_{yKapton}}{l}$$

$$C_{yKapton} = \frac{(3.5)(8.854 \times 10^{-12})(929.0304)}{0.0127}$$

Thus, the calculated capacitance of yellow Kapton is $C_{yKapton} = 22.67nF$

The measured value of the yellow Kapton using the water-filled circular ring was

$C_{yKapton} = 0.13n$

Similarly, the measured capacitance values of other test materials are shown in Table 11:

Table 11: Measured capacitance value of the test samples.

Material	Capacitance (nF)
Black Kapton	0.0383
Semi-black Kapton	0.149
Delrin	0.0184
Lexan	0.0149

CHAPTER 5: CONCLUSION AND FUTURE WORK

5.1. Thesis summary

The work presented here has reviewed the preliminary results of experiments to uniformly charge the surface of dielectric sheet samples, and, to develop a method for surface charge removal for the reduction of ESD. To achieve uniform surface charging and discharging, the following aspects were emphasized: -

   a) Geometry of a sample;

   b) Corona source voltages (positive and negative biasing);

   c) Discharge gap between the corona source and the sample;

   d) Movement of the corona source;

   e) Reading accuracy of the E-field meter;

   f) Number of passes of the brush tool (gentle/soft brushing);

   g) Ambient relative humidity (both lower and higher levels) and room temperature.

The conclusions are summarized as follows.

i.   A test stand has been constructed and utilized for the surface charge characterization and for the surface charge removal from dielectric materials at low (16-22%) and high relative humidity (>30%) in an ambient temperature environment. This test stand-

   a) This test setup allowed for uniform charging and discharging of solid dielectric sheets of area up to $\approx$ 30.5 cm $\times$ 30.5 cm (12 in. $\times$ 12 in.). (The exception is Adiprene, which was found not to charge).

b) Dielectric materials were successfully charged up to surface voltages, $V_{diel} \approx -15$ kV ($E_{diel} = -15$ kV/cm).

c) The setup was used to test six dielectric samples: black Kapton, semi-black Kapton, yellow Kapton, Lexan, white Delrin, and red Adiprene (urethane).

ii. Three different brushes (see details above) were used for surface charge removal. An audible "crackling" sound could be heard when the brush approached the charged dielectric, but no visible discharge was seen by eye or using a video camera. The best charge removal was obtained using a grounded commercial resistive brush (brush #1) with Thunderon® bristles. This brush could remove more than 90% of the surface charge from the dielectric. This seems to be true at higher V_{diel}. However, at lower voltages, (e.g. -1 kV), it appears that there may be a lower limit to the amount of charge that can be removed by brushing, corresponding to an E-field on perhaps ~ 0.5 kV/cm.

iii. Multiple brushings had modest additional effects in removing surface charge depending on the material, and in some cases increased the measured E-field, e.g. for Lexan.

iv. All tested dielectric materials were found to discharge passively with time except Lexan. The decay time constant(s) is(are) found to be a nonlinear function of the surface voltage (applied voltage).

v. Localized brushing in a 2D plane of a charged dielectric resulted in a charge distribution that suggests that each material may have a maximum ∇E that can be supported. No differences were observed in the x and y directions.

vi. A limited number of experiments on the surface resistivity were conducted on a

systematic basis to explore any correlations between the surface resistivity and surface voltage. It was found that there is no correlation between the tendency of a dielectric to charge more and the surface resistivity of the dielectric material.

vii. Detailed results are summarized in Table 12:

Table 12: Summary of experimental results.

Tested Materials	Basic Result/Comments	Range of Discharge Times [second]	Surface Resistivity [Ω/square]	Range of E-field gradient, ∇E, kV/cm^2
Red Adiprene	Did not charge	N/A	8.32×10^{10}	N/A
Black Kapton	Charged up to (-15 kV/cm) at low and high humidity, discharged E-field vs. time constant, τ	$\tau \approx 1900$ to 19,000	2.11×10^{11}	∇E ≈ 0.54 to 1.0; Average, ∇E = 0.81
Semi-black Kapton	Charged up to (-15 kV/cm) at low and higher humidity, discharged E-field vs. time constant, τ	$\tau \approx 7,500$ to 20,000	1.68×10^{11}	∇E =1.08 in x-dir; ∇E = -0.78 in y-dir
Yellow Kapton	Charged up to (-15 kV/cm) at low and higher humidity, discharged rapidly, E-field vs. time constant, τ	$\tau \approx 245$ to >900	1.42×10^{11}	∇E ≈ 0.81 to 1.5; Average, ∇E = 0.99
Lexan	Charged up to (-15kV/cm) at low and higher humidity, charge up itself, discharged E-field vs. two-time constants, τ_1, τ_2	$\tau_1 \approx 75$ to 19,000; $\tau_2 \approx 8,000$	1.02×10^{14}	∇E ≈ 0.74 to 0.87; Average, ∇E = 0.80
Delrin	Charged up to (-10 kV/cm) at low and higher humidity, discharge rapidly with single τ, would not hold charge for $V_{scr} > -10$kV	$\tau \approx 65$ (at -10 kV) to > 20,000 τ too short to measure above -10 kV	2.20×10^{13}	∇E ≈ 0.19 to 0.86; Average, ∇E = 0.58

5.2. Future work

The experimental results from this thesis can be used as a foundation for future work exploring and analyzing dielectric materials. There are some natural extensions and improvements to some experiments in this thesis that could strengthen and expand the results. The following could be areas of future work:

1. Establish an automated system to move the corona source, the electric field meter, and, the brush tool.

2. All experiments can be performed possibly with higher screen bias voltages, $V_{scr} > $ -15 kV to -30 kV.

3. The corona source can be operated with an RF discharge voltage, instead of floating DC power supply, in an effort to obtain the positive charging.

4. As the brush approaches the charged surface of the dielectric, an audible crackling is heard in the region of the brush bristle. Future work could include making high-speed movies of the manual brushing if micro discharges can be seen at the brush bristle which is closest to the dielectric surface.

5. Black/semi-black/yellow Kapton with same thickness (if available in market) could be explored to get a better understanding of this mechanism.

6. To explore the effects of temperature on surface charging, passive discharging versus time, and brush discharging for both the entire surface sample and localized brushing.

REFERENCES

[1] O. McAteer, "History of Electrostatics," in *Electrostatic Discharge Control*, New York:McGraw-Hill, 1990,ch.3, p. 426.

[2] EOS/ESD Association, Inc., "Setting the Global Standards for Static Control," 25 May 2017. [Online]. Available: https://www.esda.org.

[3] O. J. McAteer, "Introduction and Extend of the ESD Problem," in *Electrostatic discharge control*, New York:McGraw-Hill, 1990,ch.1, p. 3.

[4] D. L. Borovina, "Electrostatic Discharge Concepts and Definitions," Los Alamos National Laboratory, Los Alamos, June, 2008.

[5] EOS/ESD Association, Inc., "Fundamentals of Electrostatic Discharge," EOS/ESD Association, Inc., Rome, NY, 2013.

[6] EOS/ESD Association Inc., "Setting the Global Standards for Static Control," 26 May 2017. [Online]. Available: htp://www.esda.org.

[7] EC&M, "Electrostatic Discharge Causes Eeffects and Solutions," [Online]. Available: http://ecmweb.com. [Accessed 20 May 2017].

[8] EOS/ESD Association, Inc., "Triboelectric Charge Accumulation Testing," ESD Association, Rome, NY, 2013.

[9] EC&M, [Online]. Available: http://ecmweb.com/content/electrostatic-discharge-causes-effects-and-solutions. [Accessed 20 May 2017].

[10] EOS/ESD Association, Inc., "Triboelectric Charge Accumulation Testing," 26 May 2017. [Online]. Available: http://www.esda.org.

[11] J. Kemsley, "University of Hawaii lab explosion likely originated in electrostatic discharge," Hawaii:Chemical & Engineering News, Copyright © 2017 American Chemical Society, Volume 9, Issue 28, p. 5, July 11, 2016.

[12] P. S. Neelakanta, Handbook of Electromagnetic Materials: Monolithic and Composite Versions and Their Applications, CRC Press, 1995.

[13] F. J. Mertinez, "Explosive safety with regards to electrostatic discharge," M.S. thesis,Dept. Elect. Eng.,Univ. of NM, ABQ,NM, 2014.

[14] D. L. Borovina, "Electrostatic Discharge Concepts and Definitions," W-6, LANL, Los Alamos, June,2008.

[15] F. J. Mertinez, *Explosive safety with regards to electrostatic discharge,* ABQ,NM: M.S. thesis,Dept. Elect. Eng.,Univ. of NM, 2014.

[16] J. B. Bacon, "Electrostatic Discharge Issues in International Space Station Program EVAs," NASA Johnson Space Center, Houston, TX. [Online]. Available: http://ntrs.nasa.gov.

[17] D. K. Davies, "Charge generation on dielectric surfaces," *J. of Physics D: Applied Physics,* vol. 2, no. 11, pp. 1533-1537, 1969.

[18] J. Pierre, "Process and device to remove static electricity from plastic films". U.S. Patent 3634726 A, 11 Jan 1972.

[19] E. B. e. al., "Decay of electrical charge on polyethylene films," *J. of Physics D: Applied Physics,* vol. 10, no. 4, pp. 487-497, 1977.

[20] A. R. B. a. G. Carr, "Characteristics of propagating electrostatic discharges on dielectric films," *J. of Electrostatics,* vol. 10, pp. 321-326, May 1981.

[21] T. O. a. Y. Ito, "Studies on Electrostatic Surface Discharges on Corona-Charged Polymer Surfaces," in *IEEE Transactions on Industry Applications*, Jul/Aug 1990@IEEE,doi:10.1109/28.55990.

[22] J. A. G. a. O. N. Oliveira, "Corona Charging of Polymers," in *IEEE Transactions on Electrical Insulation*, Oct 1992@IEEE,doi:10.1109/14.256470.

[23] N. Gibson, "Static electricity — an industrial hazard under control?," *J. of Electrostatics,* Vols. 40-41, pp. 21-30, June 1997.

[24] R. M. Schaffert, Electrophotography,2nd rev. and expanded ed., London:The Focal Press,1980, 1975.

[25] P. X. e. al, "Influence of humidity on the characteristics of negative corona discharge in air," in *Physics of Plasmas*, Sep 2015@AIP,doi:10.1063/1.4931744.

[26] Mcmaster-carr, [Online]. Available: https://www.mcmaster.com. [Accessed 24 Feb 2016].

[27] Dehumidifiers USA, [Online]. Available: http://www.dehumidifiersusa.com. [Accessed 1 Mar 2016].

[28] M. A. Noras, "Non-contact surface charge/voltage measurements Fieldmeter and voltmeter methods," New York:TREK, INC., 2002.

[29] DuPont™, "Kapton® B black, homogeneous opaque polyimide film," DuPont™, [Online]. Available: http://www.dupont.com. [Accessed 23 March 2017].

[30] DuPont™, "DuPont™ Kapton® B," [Online]. Available: http://www.dupont.com. [Accessed 23 March 2017].

[31] "Kapton®Polyimide Film," McMaster-Carr, [Online]. Available:

https://www.mcmaster.com. [Accessed 23 March 2017].

[32] Plastics™,SABIC Innovative, "Lexan*XL102UV Sheet-Product Datasheet," [Online]. Available: http://www.seaworthygoods.com. [Accessed 23 March 2017].

[33] "Delrin®acetal resin," DuPont™, [Online]. Available: http://www.dupont.com. [Accessed 23 March 2017].

[34] "Prepolymers,"Adiprene direct, [Online]. Available: http://www.adiprenedirect.com. [Accessed 23 March 2017].

[35] O. J. McAteer, "Basic principles of Electrostatics," in *Electrostatic Discharge Control*, New York:McGraw-Hill Publishing Company, 1990,ch. 4, pp. 52-53.

[36] Prostat, *User Manual of PRS-812 Resistance Meter,* Bensenville, IL 60106 USA: Prostat®Corporation, 2012.

[37] O. J. McAteer, "Basic principles of electrostatics," in *Electrostatic Discharge Control*, NY:McGraw-Hill Publishing Company , 1989,ch. 4, pp. 54-55.

[38] R. E. V. a. R. Bartnikas, "Electrostatic charge measurements," in *Engineering Dielectrics*, BL:American Society for Testing and Materials, vol.IIB,ch.6,May 1987, pp. 440-489.

[39] Kapton®Dupont™, "Dupont™ Kapton®Summary of Properties," [Online]. Available: http://www.dupont.com. [Accessed 26 March 2017].